ISTANBUL TECHNICAL UNIVERSITY ★ GRADUATE SCHOOL

SYNTHESIS OF ZEOLITE A COATINGS

M.Sc. THESIS

Arzu BAYRAK

Department of Chemical Engineering

Chemical Engineering Programme

FEBRUARY 2022

ISTANBUL TECHNICAL UNIVERSITY ★ GRADUATE SCHOOL

SYNTHESIS OF ZEOLITE A COATINGS

M.Sc. THESIS

Arzu BAYRAK
(506181001)

Department of Chemical Engineering

Chemical Engineering Programme

Thesis Advisor: Prof. Dr. Ayşe ERDEM

FEBRUARY 2022

ISTANBUL TEKNİK ÜNİVERSİTESİ ★ LİSANSÜSTÜ EĞİTİM ENSTİTÜSÜ

ZEOLİT A KAPLAMALARININ SENTEZİ

YÜKSEK LİSANS TEZİ

Arzu BAYRAK
(506181001)

Kimya Mühendisliği Anabilim Dalı

Kimya Mühendisliği Programı

Tez Danışmanı: Prof. Dr. Ayşe ERDEM

ŞUBAT 2022

Arzu Bayrak, an M.Sc. student of ITU Graduate School, with the student ID 506181001, successfully defended the thesis entitled “SYNTHESIS OF ZEOLITE A COATINGS”, which she prepared after fulfilling the requirements specified in the associated legislations, before the jury whose signatures are below.

Thesis Advisor :	**Prof. Dr. AYŞE ERDEM** İstanbul Technical University	.....
Jury Members :	**Prof. Dr. Melkon TATLIER** Istanbul Technical University	.....
	Prof. Dr. İsmail BOZ Istanbul University	.....

Date of Submission : 14 January 2022
Date of Defense : 10 February 2022

To my mother,

FOREWORD

I would like to thank Prof. Dr. Ayşe Erdem and Prof. Dr. Melkon Tatlıer for their support and guidance. I would also like to thank my dear friend MSc. Chem. Eng. Taylan Maraş for his help, time, patience and friendship.

January 2022

Arzu Bayrak
(Chemical Engineer)

TABLE OF CONTENTS

Page

ABBREVIATIONS

LTA **:** Linde Type A

LTN **:** Linde Type N

TGA **:** Thermogravimetric analysis

XRD **:** X-ray diffraction

LIST OF TABLES

Page

LIST OF FIGURES

Page

SYNTHESIS OF ZEOLITE A COATINGS

SUMMARY

Zeolites are microporous crystalline hydrated aluminosilicates with pores of molecular sizes in their framework. Zeolite A is a hydrophilic synthetic zeolite with the lowest Si/Al ratio possible for zeolites, which is 1 and has a 3-dimensional pore structure with effective pore diameter about 4 Å.

During zeolite synthesis, an amorphous reactant mixture is converted into microporous crystalline product. In addition to the conventional powder and pellet forms, zeolites can be synthesized on various surfaces as coatings via different synthesis methods. These coatings may be used in separation and heating-cooling applications. Zeolite coatings prepared for use in separation applications, should be continuous thin coatings without defects.

Two new methods developed recently in our laboratory for the preparation of zeolite coatings are conduction heating and induction heating methods. The main idea of these methods is that the substrate is heated by conduction or induction and the synthesis solution is kept at a lower temperature than the surface temperature of the substrate. In this way, crystallization on the substrate is favored with respect to that in the synthesis solution. The induction heating method was observed to be suitable for use in large-scale applications. The purpose of this study is to test the applicability of the induction heating method to the preparation of thin zeolite A coatings on cylindrical metal substrates that may be suitable to be used in separation applications. The effects of different substrate types and system/synthesis parameters on the properties and performance of the synthesized zeolite A coatings are examined.

Different cylindrical metal substrates to be used in the coating experiments were designed and constructed with various types of 316L stainless steel wire mesh sheets. Zeolite A coatings were prepared by heating the metal substrate with induction power in a circulating synthesis solution system. The prepared coatings were weighed and their mass equivalent thickness values were calculated. The samples taken from the coatings were analyzed by thermogravimetric analysis (TGA) and X-ray diffraction (XRD) techniques. Nitrogen permeabilities of the coatings were also measured.

Before the synthesis experiments, the dependence of reactor inlet and outlet temperatures and thus the temperature difference obtained across the reactor on other system parameters are determined with the help of calibration experiments carried out using water instead of synthesis solution.

Zeolite A coating synthesis experiments were started by testing different substrate types, 24x110/500 (single outer layer), 24x100/500/500 (double outer layers) and 24x110/200x1400. An additional zeolite phase besides LTA, the LTN phase, was also seen to be present in smaller amounts, in the coatings obtained in these preliminary experiments. 24x110/200x1400 was observed to be the substrate type on which the most preferable coatings with lower amounts of LTN phase, and lower permeance and

thicknesses values were obtained. For this reason, zeolite A coating experiments were continued using 24x110/200x1400 substrates.

When experiments at different flow rates were conducted, it was observed that thinner and more closed coatings could be obtained using lower flow rates. For the investigation of the effects of inlet-outlet temperatures on the coating properties, experiments at different reactor inlet-outlet temperatures in the range of 30-35 to 55-60 °C, for two different synthesis times of 3 and 5 hours, were carried out. The coating thickness increased with the increase in reactor inlet and outlet temperatures, for both synthesis times. The gas permeance, however, seemed to decrease with the increase in coating thickness at low thickness values, while it started to increase again above coating thickness values of about 100 μm, for both synthesis times.

In order to optimize the effects of reactor inlet-outlet temperatures to prepare thinner coatings with lower permeabilities, running the experiment in stages with different reactor inlet-outlet temperatures was attempted and successfully achieved. The smallest equivalent thickness obtained was 210 μm for the only coating synthesized with a gas permeance value lower than 10^{-9} mol/m^2.s.Pa, in these initial two staged experiments. This coating was obtained with 3 hours of first stage at reactor inlet-outlet temperatures of 45-50°C, followed by 2 hours of second stage at reactor inlet-outlet temperatures of 55-60 °C.

Two staged synthesis approach was further investigated by keeping one of the first or second stages same and changing the reactor inlet-outlet temperatures of the other stage. The change in reactor inlet-outlet temperatures in the second stage affected the coating thickness more significantly, while it affected the gas permeance less. The effect of the temperature change of the first stage against the temperature change of the second stage was more striking. As the temperature of the first stage increased in the range tested in these experiments, both the coating thickness and the gas permeance values decreased.

The coating obtained from the experiment with the reactor inlet-outlet temperatures of 45-50 and 50-55 °C in the first and second stages, carried out for 3 and 2 hours, respectively, was observed to have an equivalent thickness value of 112 μm, almost half the value of 210 μm for the previous coating obtained at 45-50 and 55-60 °C. The actual effective thickness value of the coating across which gas permeation takes place is expected to be lower than the equivalent thickness value calculated, for the substrates used in this study. Both of these coatings had sufficiently low gas permeance values lower than 10^{-9} mol/m^2.s.Pa.

Finally, the results of XRD and TGA analyses revealed that both of these coatings were highly crystalline zeolite A coatings.

ZEOLİT A KAPLAMALARININ SENTEZİ

ÖZET

Zeolitler, mikrogözenekli, kristal yapılı, sulu alüminosilikatlardır. LTA (Linde Tip A) olarak sınıflandırılan zeolit A'nın, boşluk hacim oranı %47 ve Si/Al oranı 1'dir. Birbirlerine 8 üyeli halka denilen pencerelerle bağlanmış kafeslerden oluşan 3 boyutlu bir gözenek yapısına sahiptir. Na formunda, etkin gözenek çapı yaklaşık 4 Å'tur.

Zeolit sentezi, amorf reaktan karışımının mikro gözenekli kristal yapılı ürüne dönüşmesiyle gerçekleşmektedir. Zeolitler, cam, seramik, polimer, selüloz ve metal gibi çeşitli yüzeylerde farklı sentez yöntemleri kullanılarak kaplama olarak da sentezlenebilir. Zeolit kaplamalar kullanılarak membran uygulamaları veya ısıtma-soğutma uygulamaları gibi yeni uygulamalar geliştirilmektedir. Ayırma uygulamalarında kullanılmak üzere hazırlanan zeolit kaplamalar, kristaller arası kusurlar olmadan mükemmel şekilde iç içe geçmiş ince kaplamalar olmalıdır.

Zeolit kaplamaların hazırlanmasında en yaygın olarak kullanılan yöntemler: in-situ kristalizasyon (birincil büyüme), aşı kristalleriyle kristalizasyon (ikincil büyüme) ve bağlayıcı destekli kristalizasyondur. Birincil ve ikincil yöntemlerin mantığı, toz halindeki zeolitlerin geleneksel sentez mantığı ile aynıdır.

Birincil büyütme yöntemi, altlığın hazırlanan sentez çözeltisi ile doğrudan temas halinde olduğu hidrotermal sentez yöntemidir. Sentez sistemi kesikli, yarı-sürekli veya sürekli bir sistem olabilir. Kesikli sistemlerdeki sorunlardan biri, jel ve kristallerin çözeltide çökmesi ve belirli noktalarda birikmesidir. Sürekli sistemlerde, sirkülasyonla hareket halinde olan sentez çözeltisinin tüm altlığa teması, jel ve kristallerin çökelmesini ve birikmesini önler. Aynı zamanda sürekli sistemler, kesikli sistemlere kıyasla ölçek büyütmede daha avantajlıdır.

İkincil büyütme yönteminde, altlık, hidrotermal sentezden önce çeşitli yöntemler kullanılarak zeolit kristalleri ile aşılanır. Aşılama aşaması sırasında kristal boyutu, kristal yoğunluğu ve biriktirme süresi gibi birçok parametre vardır. Aşı kristallerinin homojen ve sürekli bir şekilde altlık üzerine yerleştirilmesi, sentez sonrası hazırlanan ince kaplamanın homojen bir kalınlığa ve hatasız bir yapıya sahip olmasını sağlar. Aşılama ayrıca sentez süresini kısaltır ve kristal büyümesinin sentez çözeltisinden ziyade altlık üzerinde gerçekleşmesini teşvik eder.

Son zamanlarda bölümümüz laboratuvarlarında metal altlıkların kondüksiyon veya indüksiyon yoluyla seçici olarak ısıtılmasıyla zeolit kaplamaların hazırlanması için iki yöntem geliştirilmiştir. Bu çalışmanın amacı, mümkünse silindirik metal altlıklar üzerinde ayırma amaçlı olarak kullanıma uygun olabilecek ince zeolit A kaplamalarının hazırlanmasında indüksiyonla ısıtma yönteminin uygulanabilirliğinin araştırılmasıdır. Altlık tipi ve sistem/sentez parametrelerinin sentezlenen zeolit A kaplamasının özellikleri ve performansı üzerindeki etkileri incelenmiştir.

Kaplama deneylerinde kullanılan katmanlı silindirik metal altlıklar, çeşitli tiplerde 316L paslanmaz çelik elekler kullanılarak tasarlanmış ve üretilmiştir. İç katman için

seçilen elek levha istenilen ebatlarda dikdörtgen şeklinde kesilerek, uzun kenarları birbirine kaynak yapılarak bir silindir oluşturulmuştur. Dış katman için seçilen elek levha daha sonra bu silindirin etrafına sarılarak ve uzun kenarları boyunca birleştirilerek kaynak yapılmıştır. Son bir adım olarak, silindirin her iki ucuna metal halkalar kaynaklanmıştır. Kaynak hatlarındaki deformasyonları kapatmak için metal altlığın yanal bölgesindeki kaynak hattına ve halka birleşim alanına ince birer epoksi şeridi uygulanmıştır.

Zeolit A kaplamalar, metal altlığın, berrak bir sentez çözeltisinin sirküle edildiği bir reaksiyon sisteminde indüksiyon gücüyle ısıtılmasıyla hazırlanmıştır. Sistemde pompadan geçen çözelti reaktöre girmekte, reaktörden çıktıktan sonra kreostattan geçerek pompaya geri dönmekte, ardından tekrar reaktöre iletilmekte ve böylece sirkülasyon sağlanmaktadır. Reaktörde silindirik metal altlığın hem içinden hem de dışından geçen reaksiyon karışımı, reaktörden çıkmadan önce altlığın ısıtılan yüzeyleriyle temas etmesi sonucu bir dereceye kadar ısınmakta ve daha sonra kreostattan geçerek tekrar soğutulmaktadır. Deney sırasında reaktör giriş-çıkış sıcaklıkları ısıl çiftler ile izlenmiştir ve kreostat sıcaklığı ve indüksiyon gücü ayarlanarak istenilen sıcaklık değerlerinde tutulmuştur. Belirli koşullarda seçilen süre sonunda reaktörden çıkarılan zeolit kaplı metal altlık, distile su ile durulanmış ve kontrollü nemli bir ortamda tutulmuştur. Tartımları izlenen kaplamalardan alınan numuneler, termogravimetrik analiz (TGA) ve X-ışını kırınımı (XRD) teknikleri ile analiz edilmiştir. Kaplama miktarlarından kütlece eşdeğer kaplama kalınlıkları hesaplanmıştır. Eleklerin boşluklarındaki etkin kalınlık değerlerinin eşdeğer kalınlık değerlerinden çok daha düşük olması beklense de, hesapla bulunan bu değerlerden, geçirgenliği düşük ve olabildiğince ince kaplamalar hazırlanması için yol gösterici olarak yararlanılmıştır. Kaplamalardan altlıkları uygun olanların azot geçirgenlikleri ölçülmüştür.

Sentez deneylerine başlamadan önce, sentez çözeltisi yerine su kullanılarak kalibrasyon deneyleri yapılmıştır. İndüksiyon gücü, kreostat sıcaklığı ve debi parametreleri değiştirilerek reaktör giriş ve çıkış sıcaklıklarına ve dolayısıyla reaktör genelinde elde edilen sıcaklık farkına etkileri belirlenmiştir. Kalibrasyon deneyleri sonucunda indüksiyon gücündeki artışın reaktör giriş ve çıkış sıcaklıkları arasındaki farkı arttırdığı gözlemlenmiştir. Kreostat sıcaklığı arttığında hem reaktör giriş hem de çıkış sıcaklıklarının arttığı gözlemlenmiştir. Debinin artmasıyla giriş sıcaklığının arttığı ancak çıkış sıcaklığının azaldığı yani reaktör giriş ve çıkış sıcaklıkları arasındaki farkın azaldığı gözlemlenmiştir. Sistemde farklı tipte metal altlıklar kullanıldığında, aynı reaktör giriş ve çıkış sıcaklıklarını bulmak için farklı deneysel parametrelerin uygulanmasının gerektiği görülmüştür.

Zeolit A kaplama sentezi deneyleri, 24x110/500 ve 24x100/500/500 olmak üzere iki farklı altlık türü test edilerek başlatılmıştır. Sentez süresi arttıkça kaplama miktarının ve dolayısıyla kalınlığının arttığı görülmüştür. Bu altlıklarla yapılan deneylerde, iç ve dış yüzeylerden kazınan numunelerin XRD'leri incelenmiştir.

24x110/500 altlık ile hazırlanan kaplamalarda LTA fazının yanısıra, daha az miktarlarda da olsa LTN fazına da rastlanmıştır. Üç saatlik sentezden sonra elde edilen kaplamanın iç ve dış yüzeylerinden alınan numunelerin XRD sonuçları incelendiğinde, iç taraftan alınan numunenin XRD'sinde LTN piklerinin daha yüksek olduğu görülmüştür. Öte yandan, 5 saatlik sentezden sonra elde edilen kaplamanın iç ve dış yüzeylerinden alınan numuneler incelendiğinde, numuneler arasında önemli bir fark görülmemiştir.

Bu deneylerden elde edilen kaplanmış altlıkların dış yüzeylerinden alınan numunelerin XRD sonuçları incelendiğinde, dış yüzeyde LTN oluşumunun zamanla arttığı görülmüştür. Kaplamanın bu tarafında daha önce LTN fazının mevcut olmadığı gözlenmiştir. İç yüzeylerden elde edilen iki örneğin XRD grafikleri arasında önemli bir fark olmadığı, her iki grafikte de LTN piklerinin bulunduğu saptanmış, LTN'nin iç yüzeyde daha erken bir zamanda oluştuğu görülmüştür.

24x110/500/500 altlık ile hazırlanan kaplamalarda, üç saatlik sentez sonrası elde edilen kaplamanın iç ve dış yüzeylerinden alınan numunelerin XRD sonuçları karşılaştırıldığında, numuneler arasında önemli bir fark gözlenmemiştir. Öte yandan, 5 saatlik sentezden sonra elde edilen kaplamanın iç ve dış yüzeylerinden alınan numunelerin XRD grafikleri incelendiğinde, dış tabakadan alınan numunenin XRD'sinde LTN piklerinin biraz daha yüksek olduğu görülmüştür.

Kaplanmış altlığın hem iç hem de dış yüzeylerinden alınan numunelerde LTN fazını gösteren piklerin zamanla arttığı gözlemlenmiştir. Artış, kaplamanın dış yüzeyinde daha belirgindir. Bu sonuçlar, LTN fazının, zeolit A pahasına sentez süresi ile arttığını göstermektedir.

Tek ve çift katmanlı 500 mesh ile hazırlanan altlıklar karşılaştırıldığında, iç yüzeylerden alınan numuneler arasındaki farklılıkların pek belirgin olmadığı, ancak kaplamaların dış yüzeylerinden alınan numunelerdeki LTN piklerinin 24x110/500/500 altlığında 24x110/500 altlığına göre daha yüksek olduğu belirlenmiştir.

Bu aşamada, kaynak işleminde yapılan birkaç iyileştirme ile şekilsel düzgünlük açısından iyileştirilmiş altlıklar üretilmeye ve kullanılmaya başlanmıştır. Bu sayede hazırlanan kaplamaların gaz geçirgenlik ölçümleri ile test edilmesi mümkün hale gelmiştir. Hazırlanan kaplamaların ne kadar sürekli ve kapalı olduğunu test etmek için azot geçirgenlik ölçümleri yapılmıştır.

Tek bir dış tabakanın kullanımına karar verildikten sonra, dışta 200x1400 mikronik elek türünün kullanıldığı üçüncü bir altlık türü geliştirilmiştir. 24x110/500 ve 24x110/200x1400 altlık türlerinin kıyaslanması amacıyla sentez deneyleri yapılmıştır. İki altlık tipi ile elde edilen kaplama kalınlıkları arasında belirgin bir fark görülmemiştir. Ancak 24x110/200x1400 altlık tipinde hazırlanan kaplamaların biraz daha düşük gaz geçirgenlik değerleri vermesi, bu altlık ile elde edilen kaplamaların daha kapalı olduğunu göstermiş ve zeolit A kaplama deneylerine 24x110/200x1400 altlık türü kullanılarak devam edilmiştir.

Farklı debilerin etkisini incelemek ve sonraki deneyler için uygun bir akış hızı seçmek için 74.8, 149.6 ve 224.4 ml/dak olmak üzere üç debi seçilmiştir. Azalan debi ile birlikte sistemin indüksiyon güç ihtiyacının azalması kaplama miktarının azalmasına neden olmuştur. Daha düşük akış hızı kullanılarak, altlık üzerinde daha ince ve daha kapalı kaplamalar elde edilebilmiştir.

Reaktör giriş ve çıkış sıcaklıkların kaplama özellikleri üzerindeki etkilerini araştırmak ve değerlerini optimize etmek için bir dizi deney planlanmış ve gerçekleştirilmiştir. 35 ve 40 °C'den 55 ve 60 °C'ye kadar farklı reaktör giriş ve çıkış sıcaklıklarında 74,8 ml/dak debide 3 saatlik sentez deneyleri yapılmıştır. Reaktör giriş ve çıkış sıcaklıklarının artmasıyla kaplama kalınlığı artmıştır. Gaz geçirgenliği ise düşük kalınlık değerlerinde kaplama kalınlığının artmasıyla azalırken, yaklaşık 100 µm kaplama kalınlık değerlerinin üzerinde tekrar yükselmeye başlamıştır. Bu nedenle, 30-35 °C ila 50-55 °C arasında 5 saatlik sentez deneylerinden oluşan başka bir dizi deney yapılmıştır. Bu deneylerde de sıcaklıkların artışıyla kaplama kalınlığı artarken, en

düşük gaz geçirgenlik değerlerinin yine 100 μm civarında bir optimum kalınlık değerinde elde edildiği görülmüştür.

Kalınlığı artırmadan geçirgenliği düşürmek için çok aşamalı kaplama deneyleri yapılmıştır. Deneyin ilk aşamasında, daha düşük reaktör giriş-çıkış sıcaklıkları ile çekirdeklenmenin yavaş gerçekleşmesini sağlamak, ikinci aşamada ise reaktör giriş-çıkış sıcaklıklarını artırarak kristalleşmeyi hızlandırmak amaçlanmıştır. Bu deneyler, 45-50 °C'lik reaktör giriş-çıkış sıcaklıklarında 3 saatlik bir birinci aşamanın ardından, 55-60 °C'lik reaktör giriş-çıkış sıcaklıklarında 1 veya 2 saatlik ikinci aşama uygulanarak yürütülmüştür. Bu deneylerin sonuçlarını değerlendirebilmek için, 45-50 °C reaktör giriş-çıkış sıcaklıklarında 3 saat boyunca ikinci bir aşama olmaksızın yapılan deneyin sonuçları ile karşılaştırılma yapılmıştır. Reaktör giriş-çıkış sıcaklıklarının 10 °C yükseltilip deneye 1 saat daha devam edilmesinin bile gaz geçirgenliğini ciddi ölçüde azalttığı görülmüştür. İkinci aşama iki saate uzatıldığında ise azot geçirgenliği 10^{-9} mol/m^2.s.Pa değerinin altına düşmüştür. Çalışmada bu aşamaya kadar gözlenen en düşük geçirgenliğe sahip olan bu kaplamanın (A28 kodlu deney) eşdeğer kalınlığı 210 μm olarak hesaplanmıştır.

İki aşamalı sentez yaklaşımı, 3 saatlik ilk aşama ve 2 saatlik ikinci aşama kullanılarak ve birinci veya ikinci aşamalardan biri aynı tutularak ve diğer aşamanın reaktör giriş-çıkış sıcaklıkları değiştirilerek daha detaylı araştırılmıştır. İlk olarak, reaktör giriş-çıkış sıcaklıkları ilk aşamada 40-45 °C gibi daha düşük bir değerde tutulmuştur. İkinci aşamalarında ise 45-50, 50-55 ve 55-60 °C reaktör giriş-çıkış sıcaklıklarında deney gerçekleştirilmiştir. İkinci aşamada reaktör giriş-çıkış sıcaklığındaki değişim kaplama kalınlığını daha fazla, gaz geçirgenliğini ise daha az etkilemiştir.

İki aşamalı deneyler kapsamında, birinci aşamadaki reaktör giriş-çıkış sıcaklığının değişiminin etkisini gözlemlemek için de deneyler yapılmıştır. Bu deneylerin ikinci aşamaları, 50-55 °C reaktör giriş-çıkış sıcaklıklarında, ilk aşamaları ise 35-40, 40-45 ve 45-50 °C reaktör giriş-çıkış sıcaklıklarında gerçekleştirilmiştir. Birinci aşamanın sıcaklık değişiminin ikinci aşamanın sıcaklık değişimlerine göre etkisinin daha fazla olduğu görülmüştür. Bu deneylerde test edilen aralıkta birinci kademenin sıcaklığı arttıkça hem kaplama kalınlığının hem de gaz geçirgenlik değerlerinin azalması sağlanmıştır.

Sonuç olarak, ilk aşaması 45-50, ikinci aşamasıysa 50-55 °C reaktör giriş-çıkış sıcaklıklarında gerçekleştirilen (A33 kodlu) deney ile elde edilen kaplamanın, yeterince küçük (10^{-9} mol/m^2.s.Pa'dan düşük) bir gaz geçirgenlik değerine sahip olduğu ve eşdeğer kalınlık değerinin de önceden hazırlanabilmiş düşük geçirgenliğe sahip A28 kodlu kaplamanın kalınlığının neredeyse yarısına düşürülebildiği belirlenmiştir. Elde edilen eşdeğer kalınlık A28 kodlu kaplama için 210 μm iken, A33 kodlu kaplama için 112 μm'dir. Kullanılan altlıklar için eleklerin boşluklarındaki etkin kalınlık değerlerinin eşdeğer kalınlık değerlerinden çok daha düşük olması beklenmektedir.

XRD ve TGA sonuçları incelendiğinde her iki kaplamanın da yüksek kristaliniteye sahip zeolit A kaplamaları oldukları görülmüştür.

1. INTRODUCTION

Zeolites are microporous crystalline hydrated aluminosilicates with pores and channels in their framework. They can be found in nature as well as synthesized in the laboratory [1]. There are about 40 types of zeolites found in the nature and more than 200 types of zeolites synthesized in the laboratory [2]. Because zeolites found in nature contain impurities in their structures and may not have the desired pore sizes, they are not suitable for use in some industrial applications. Zeolites, which are produced synthetically in laboratories, are more commonly used in industry because they can be produced with desired properties in accordance with their usage areas.

Zeolite coatings are prepared by bonding zeolites to a substrate with physical or chemical bonds. Zeolite coatings, similar to zeolites in powder or pellet forms, can be used in adsorption, separation and catalysis applications. In some application areas, they perform much better than zeolites in powder or pellet forms due to reduced mass and heat transfer limitations [3]. Zeolite coatings can be synthesized directly on the substrate surfaces using different methods such as in situ crystallization, seed assisted crystallization and binder assisted crystallization [4].

1.1 Purpose of Thesis

Two methods have been developed recently in the laboratories of our department, for the preparation of zeolite coatings by selective heating of the metal substrates directly by conduction or induction [5, 6]. Synthesis by induction heating method has been successfully applied for the preparation of relatively thick zeolite X and zeolite A coatings on large substrate surfaces [7]. The purpose of this study is to test the applicability of the induction heating method to the preparation of thinner zeolite A coatings on cylindrical metal substrates that may be suitable for use in separation applications, if possible. The effects of substrate type and system/synthesis parameters on the properties and performance of the synthesized zeolite A coating are examined.

2. ZEOLITES AND ZEOLITE COATINGS

2.1 Zeolites

Zeolites are hydrated crystalline materials formed by silica (SiO_4) and alumina (AlO_4) tetrahedra. Each tetrahedron has a T (Si and Al) atom at the center and four oxygens at the corners. When tetrahedra are connected to each other with oxygen atoms, a 3-dimensional structure emerges. This three-dimensional network contains pores in shape of cages and channels [1]. Due to these pores in the structure, ions and molecules with an effective diameter smaller than the pore size can easily pass through the zeolite structure. Zeolites are also known as molecular sieves due to this property [8].

The silica tetrahedra in the structure with Si^{+4} at the center are neutral with four oxygens, while alumina tetrahedra with Al^{+3} at the center are negatively charged. This negative charge is neutralized with cations in the pores of the structure. Because of these cations, zeolites are frequently used in ion exchange applications [9].

The structural formula of a zeolite is represented by:

$$Mx/n[AlO2)x(SiO2)y].wH2O. \quad (2.1)$$

In the above formula, M is an alkaline (Na^+, K^+, Li^+) or alkaline earth (Mg^{+2}, Ca^{+2}, Ba^{+2}) metal cation, n is the valence of cation M, w is the number of water molecules per unit cell, and x and y are the numbers of alumina and silica tetrahedra per unit cell.

2.2 Zeolite A

Zeolite A, classified as LTA (Linde Type A), has a structural formula $Na_{12}[(AlO_2)_{12}(SiO_2)_{12}].27H_2O$ [2]. Zeolite A has a void volume fraction of 47% and Si/Al ratio of 1. It is the zeolite with the lowest possible Si/Al ratio. It has a 3-dimensional pore structure with 8 membered ring windows. In Na form, the effective pore diameter is about 4 Å. When sodium cations in its structure are exchanged with other smaller or larger cations its pore size changes. For example, its K and Ca exchanged forms, zeolites K-A and Ca-A have effective pore sizes of about 3Å and 5 Å, respectively [10].

Figure 2.1 shows the framework structure of zeolite A. The primitive structural unit of zeolite A structure is β cage. In the LTA type structure, the β cages are interconnected by double 4-membered rings and are arranged in a simple cubic structure. Then, α cages (supercages) are formed between the β cages. The α cages are linked by sharing the 8-membered ring with each other, and these structures are arranged in a simple cubic structure [11].

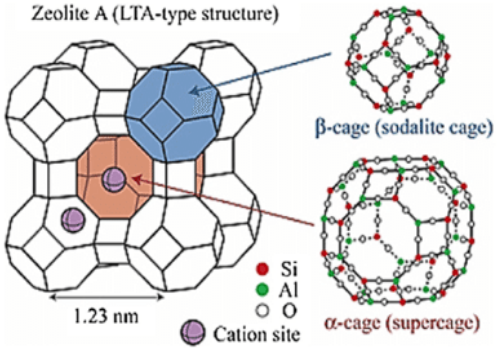

Figure 2.1 : Zeolite A framework structure [11].

2.2.1 Synthesis of zeolite A

Zeolites can be synthesized from gels or clear reaction mixtures. Various zeolites in powder form could be obtained by conventional zeolite synthesis using aluminosilicate gels. Zeolite synthesis allows the initial amorphous reactant mixture to be converted into a microporous crystalline final product. The synthesis of the structure takes place in an aqueous medium, in hydrothermal conditions (100°C - 200°C), in the presence of organic or inorganic cations. Many of the low-silica zeolites containing aluminum are synthesized using alumina and silica sources and hydroxides of alkali metal cations and water.

There are many different variables that influence the synthesis and determine the properties of the final crystal structure to be formed [12]. Among them, the most important ones are the reaction mixture composition (Si/Al ratio, water content, alkalinity, type and amount of cation(s)), temperature, synthesis time and presence of mixing [13]. The reaction accelerates with the decrease of the H_2O/Na_2O and SiO_2/Al_2O_3 ratios of the synthesis solution, and the reaction slows down with their increase. Changing the Na_2O/SiO_2 ratio of the synthesis solution has the opposite effect, with the increase of Na_2O/SiO_2 ratio, the reaction accelerates, and with the

decrease of this ratio, the reaction slows down. Increasing the reaction temperature also accelerates the reaction. Prolongation of the reaction time leads to metastable phase transformations causing an increase in the amount of hydroxysodalite, which is a more stable phase, after longer synthesis times [14].

However, the gel compositions used in these syntheses are not suitable for the preparation of zeolite coatings. New applications such as membrane applications or heating-cooling applications are being developed using zeolite coatings [15, 16]. In preparing zeolite coatings, it was observed to be better to use clear solution compositions. However, the number of known clear solution compositions which can be used in preparing the coatings is very limited. There is only one study in the literature on clear solution compositions that can be used for the synthesis of zeolite A [17]. In this study, different synthesis compositions and times at different temperatures for the synthesis of pure and fully crystalline zeolite A were investigated and the results were reported to be 3-9 hours at 60 °C, 1-5 hours at 80 °C, 1-2 hours at 90 °C, and 30 minutes at 100 °C for the composition $50Na_2O$: $1Al_2O_3$: $5SiO_2$:$1000H_2O$. Phase transformation starts after 10 hours at 60 °C, 6 hours at 80 °C, 3 hours at 90 °C, and 1 hour at 100 °C. When these synthesis times are exceeded, zeolite X and/or hydroxysodalite are formed besides zeolite A [17].

2.3 Zeolite Coatings

Zeolites can be synthesized on various surfaces such as glass, ceramic, polymer, cellulose and metal as coatings using different synthesis methods. Zeolite coatings, which have the properties of zeolites such as adsorption, catalysis and molecular sieving, provide the opportunity for them to be used in many areas [18].

In recent years, preparation of zeolite coatings on porous substrates that can be used as membranes for gas and liquid separations has been attracting a lot of attention. Zeolite coatings that will be used in adsorption applications, are expected to be sufficiently thick and continuity of the coating is not very critical in these cases. Zeolite coatings prepared for use in separation applications, on the other hand, should be perfectly intergrown thin coatings without inter-crystalline defects. When the zeolite coatings are prepared for use in sensor or microreactor applications, it may be desired that the zeolite layer consists of crystals attached to the substrate separately or as a

monolayer. Contrary to the coatings prepared for membrane applications, zeolite intergrowth is not desirable in these cases [19].

2.3.1 Preparation of zeolite coatings

Due to the advantages of zeolite coatings in many application areas, research related to the preparation of zeolite coatings has increased. The most commonly used methods in the preparation of zeolite coatings are: in situ crystallization (primary growth), seed assisted crystallization (secondary growth) and binder assisted crystallization [4].

The logic of the primary and secondary methods is the same as the traditional synthesis logic of zeolites in powder form (Figure 2.2). The primary growth method is the hydrothermal synthesis method in which the substrate is in direct contact with the prepared synthesis solution. Synthesis system can be a batch, semi-continous or continuous system. In the secondary growth method, substrate is seeded with zeolite crystals using various methods before hydrothermal synthesis [20].

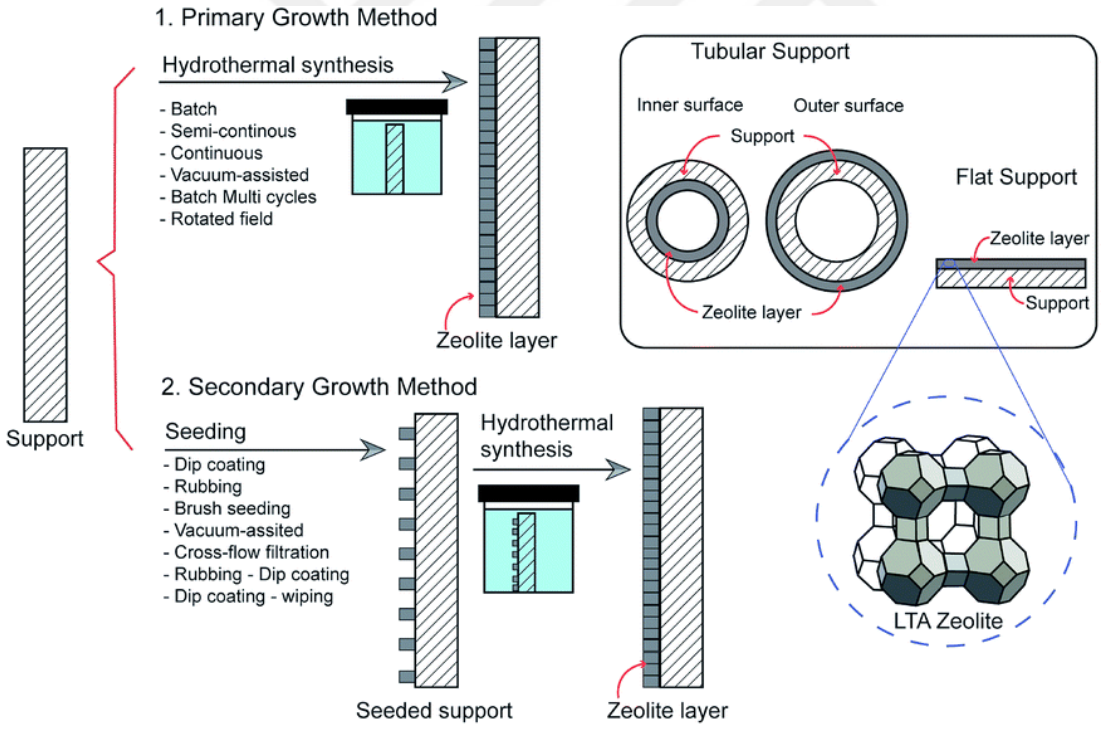

Figure 2.2 : Primary and secondary growth methods [20].

For primary growth, several approaches have been studied, such as primary growth in batch, continuous, or semi-continuous modes. In the batch system, the porous support is dipped and stabilized in the synthesis solution and heated for a certain amount of time. After this specific time, the support is removed from the solution and dipped in

a new synthesis solution in an inverted position [21]. In another method, before hydrothermal synthesis, the support goes through various pretreatment steps. The supports were immersed in organic modifiers and calcined at high temperatures in order to remove the organic phase. It has been seen that there is no need for the application of seeding with such preliminary improvement steps [22].

One of the problems in batch systems is that the reactant settles in the solution and accumulates at certain points. One of the methods developed to overcome this problem is the use of continuous flow systems. The uniform contact of the synthesis solution, which is in motion with the circulation, to the entire substrate prevents the precipitation and depletion of the reactant. At the same time, continuous systems are more advantageous in scale-up compared to batch systems [23].

Generally, in hydrothermal synthesis, heating is done by conventional methods, and this is usually done by immersing the synthesis solution and substrate into an autoclave and then heating the autoclave in an oven or hot water bath. Another heating method is microwave heating [24]. In coatings obtained with this type of heating, the discontinuity of the coating and very small crystal size are the biggest problems, so aging the synthesis solution before the synthesis or combined convectional/microwave heating method is more preferred [24, 25].

When the results of these studies are examined, it is seen that the coatings obtained using only hydrothermal synthesis have an inhomogeneous appearance. For this reason, the secondary growth method is generally used. Seeds are deposited on the substrate with different methods of seeding before hydrothermal synthesis. There are many parameters such as crystal size, crystal density, and deposit time during the seeding step [22]. In the seeding step, the seeds placed on the substrate act as nuclei during the synthesis, guiding the growth of the zeolite layer. Placing the seeds in a homogeneous and continuous manner ensures that the thin coating prepared after the synthesis has a homogeneous thickness and a defect-free structure. Seeding also shortens the synthesis time and encourages crystal growth on the substrate rather than in synthesis solution [26, 27].

The simplest seeding method is the dip coating method. In this method, the substrate is immersed in the suspension prepared with zeolite crystals and water at a certain speed, and it is left for a certain period of time and removed at a certain speed. The

biggest disadvantages of this method are that it is not reproducible and it is very difficult to obtain a homogeneous seed layer [28, 29].

Another simple seeding method is the rub-coating method. In this method, zeolite crystals are rubbed on the substrate and then synthesis is carried out with this seeded substrate. The disadvantage of this method is that a homogeneous coating cannot be obtained as a result of regional shedding of the seeds and obtained coatings are not reproducible [21, 30]. Rub-coating method is also done with a paste prepared with water and seed. This prepared paste can be applied to the surface as a thin layer and the coating can be synthesized by dipping this substrate into the synthesis solution [29].

Another seeding method is the vacuum-assisted seeding method. In this method, vacuum filtration system is used. The cylindrical substrate is immersed in a mixture containing water and seed, and a vacuum pump is attached to one end of the substrate. At this stage, as the water passes through the pores, the seeds are carried to the surface and remain there. With this technique, homogeneous distribution of seeds on the surface is easier and more reproducible than previous seeding methods [30].

One of the most important problems in the seeding step is choosing the seed size suitable for the substrate pore size. Very large seeds result in nonhomogenous coating layer. For this reason, nanocrystals are preferred [31]. Obtaining nanocrystalline zeolites is very difficult and costly. Generally, their synthesis is carried out using organic structure-directing agents or by microwave heating method [22, 32].

Two new methods developed recently in our laboratories for the preparation of zeolite coatings are conduction heating and induction heating methods. The main idea of these methods is that the substrate is heated by conduction or induction and the synthesis solution is kept at a lower temperature than the surface temperature of the substrate. In this way, crystallization on the substrate is favored with respect to that in the synthesis solution. The combination of continuous synthesis with induction heating method is a factor that increases its usability in large-scale applications [6, 7].

2.3.2 Membrane applications of zeolite coatings

Almost every process in such areas of industry as chemical, pharmaceutical, food, etc., includes the stage of separating the components according to the composition of mixtures. Today, membrane technology competes with many traditional separation

methods and is increasingly being used. Among the advantages of using membranes are mild conditions required for the separation process, its continuity, the absence of additional reagents, and perhaps the most important feature is low energy costs [33].

The creation and application of zeolite membranes is a promising direction in the development of membrane technologies. Zeolites are porous crystalline aluminosilicates with a uniform system of channels with diameters in the range of 0.3 to 2 nm, which makes them unique for the production of membrane materials. The molecular sieve action, along with tailorable adsorption characteristics, makes it possible to obtain high fluxes through the zeolite layer and a high separation selectivity, depending on the size, and the adsorption capacity for the components of the mixture. Zeolites are resistant to elevated temperatures and organic media, which expands their range of applications in comparison, for example, with polymeric membranes [34].

The main direction of application of zeolite membrane materials is the gas-phase or pervaporation separation of mixtures. So, zeolite membranes can be used for the separation of mixtures that have close boiling points, for the separation of isomeric molecules, as well as compounds that form azeotropic compositions [35]. On the other hand, zeolite membranes can be used to increase the efficiency of catalytic processes; they perform various functions, in particular, selective removal of products from the reaction zone or direct participation in catalytic reactions [36]. However, the use of zeolite membranes in this area is limited by the possibility of a presence of differences in the coefficients of thermal expansion of the zeolite layer and the substrate, which leads to the formation of defects in the zeolite layer and, as a consequence, to a decrease in the separation selectivity. Therefore, the creation of improved zeolite membranes is an urgent requirement.

Zeolite membranes of the Na-LTA structure have recently become widespread and are actively used for the separation of aqueous-organic mixtures and in catalytic membrane reactors. The main properties that determine the choice of this zeolite are its high hydrophilicity and crystal lattice with a three-dimensional pore system with a diameter of 4.1 Å, which is larger than the kinetic diameter of a water molecule, but smaller than the diameter of most organic molecules. The advantages of zeolite membranes in general are their high mechanical strength, thermal stability, and greater resistance to organic solvents in comparison with polymeric membranes. All these

properties make Na-LTA a promising membrane material for the dehydration of various mixtures.

Recently, a large number of studies have been devoted to the development of a technological procedure for the synthesis of a defect-free zeolite layer on various substrates. Due to the difficulty of obtaining a homogeneous layer of zeolite of optimal thickness, in most cases, specially polished or modified fine-pored substrates are used, which significantly increases the cost of production of selective membranes. Therefore, the task of finding a method for obtaining a selective membrane of the Na-LTA structure on large-pore industrial substrates is urgent and important.

3. EXPERIMENTAL STUDY

3.1 Preparation of Metal Substrates

The single or multi-layered cylindrical metal substrates used in the coating experiments were designed and constructed using various types of 316L stainless steel wire mesh sheets [37]. For the cylindrical metal substrates designed with two or three layers of metal sheets, a relatively more rigid and stronger mesh sheet was used as the inner layer of the cylinder. In the reactor used for synthesis and the module used for gas permeation test, the cylindrical substrate is firmly fixed from the top and the bottom and it is desired that the pressure created by this fixation does not disturb the cylindrical form of the substrate. It has been observed that the cylindrical form of the substrate was deformed when the inner wire mesh sheet was relatively thin (Figure 3.1).

Figure 3.1 : Substrates that are deformed due to the use of a relatively thin metal sheet layer on the inside.

On the outer side of the metal substrates, one or two layers of thinner wire mesh sheets were used. These thinner wire mesh sheets with smaller pore openings were preferred in order to obtain relatively thin and closed zeolite coatings. It is expected that it will be easier for the zeolite layer to close the openings between the wires without having to become too thick, when the opening size is smaller.

For the production of metal substrates, chosen wire mesh sheets were cut into rectangle shapes in desired sizes. Initially, longer edges of the wire mesh sheet chosen for the inner layer were welded to each other to form a cylinder. The wire mesh sheet chosen for the outer layer was then wrapped around this cylinder and welded to join along its longer edges. As a final step, metal rings were welded to both ends of the cylinder.

The prepared cylindrical metal substrates are 12 cm in length and 1.2 cm in diameter. This length includes the two 1 cm rings welded to each end of the 10 cm long main section of the substrate. All of the materials used are SS 316L stainless steel. Pipes with 0.2 cm wall thickness and 1.2 cm outer diameter are used for rings. For all substrates in this study, 24x110 micronic mesh sheet is preferred for the inner layer. This mesh sheet has 80 μm openings between its wires and it is chosen as the inner layer because it gives a sufficiently strong and rigid structure to the substrate, and this rigidness prevents the substrate from flexing and losing its cylindrical form in the synthesis reactor and in the gas permeation test module. Two different mesh sheets are used as the outer layer, 500 mesh sheet and 200x1400 micronic mesh sheet. 500 mesh sheet has 25 μm openings between its wires and 200x1400 micronic mesh sheet has 10 μm openings. Both mesh sheets used as outer layer have more delicate structures compared to the inner layer. In this study, 3 different substrate designs with an inner layer of 24x100 micronic mesh sheet were used. These are the 24x110/500 substrate which has a single layer of 500 mesh sheet as the outer layer, the 24x110/500/500 substrate with two layers of 500 mesh sheets on the outside, and the 24x110/200x1400 substrate with a single 200x1400 mesh sheet as the outer layer.

In some cases, deformations were observed to form along the welding lines on the lateral area and where metal rings were connected. In order for gas permeation test to accurately determine the defects in the zeolite coating on the metal substrate, these deformations that occurred during the welding had to be eliminated. For this purpose, initially it was tried to cover the welded parts of the substrate with an additionally welded thin metal plate. The metal plate placed did some good in covering the deformations, but reduced the effective surface area. At the same time, the power required to heat the metal substrate has pushed the power limits of our induction device. As the next step, use of epoxy has been tried. The main criteria in the selection of epoxy were that it should be sufficiently low in viscosity for easy application, and be resistant to the temperature and alkaline environment of the experiment. During the

experiment, the metal substrate in the reactor is heated by induction. Likewise, the metal substrate is in contact with the alkaline synthesis solution throughout the experiment. For this reason, it is desired that the physical and chemical structure of the epoxy used do not change with temperature and alkaline environment. The selected epoxy was applied on the metal substrate and observed by keeping it in the 50°C synthesis solution [38]. It was observed that the color, texture and weight of the epoxy did not change in these environments. For its resistance to temperature, the epoxy coated metal base was kept in the oven for one night and observed. After examining the properties obtained from the manufacturer, it was determined that the epoxy was suitable for use. A thin strip of epoxy was applied to the weld line on the lateral area and on the ring-substrate joint area of the metal substrate. Uncoated metal substrate and epoxy coated metal substrate weights were noted for every substrate, and the amount of epoxy used for each substrate was recorded.

The zeolite layer synthesized on the wire meshes used in a prepared substrates is not expected to be of the same thickness throughout the entire mesh opening. The crystals start to grow after nucleation on the wires and they are required to continue growing first to form layers on the wires and then until these layers growing on the wires around any mesh opening get thick enough to join in the middle of the opening to fully close the opening between the wires. It will therefore, not be possible to talk about a uniform coating thickness across any mesh opening. The growth of zeolite crystals will also be in every direction, not only in the direction of the openings between the wires. Throughout this study, coating thickness calculations were made simply by assuming that the coating was uniformly distributed as a compact zeolite layer over the cylinder surface. The thickness values reported in the study are thus, mass equivalent thickness values calculated for corresponding compact zeolite coatings of equal mass on the planar lateral (curved) surfaces of tubular supports of same diameter. These values, therefore, do not correspond to actual thickness values. They are only used as indicators to optimize the synthesis conditions in order to prepare thinner coatings with lower permeabilities. The actual thickness value of the coating across which gas permeation takes place is expected to be much lower than the equivalent thickness value for the substrates used in this study.

3.2 Synthesis Experiments

Zeolite A coatings are prepared by heating the metal substrate with induction power in a circulating synthesis solution system. The experimental setup contains an induction device, a reactor inside an induction coil, a peristaltic pump, a cryostatic water bath, two thermocouples, pipeline and valves (Figure 3.2).

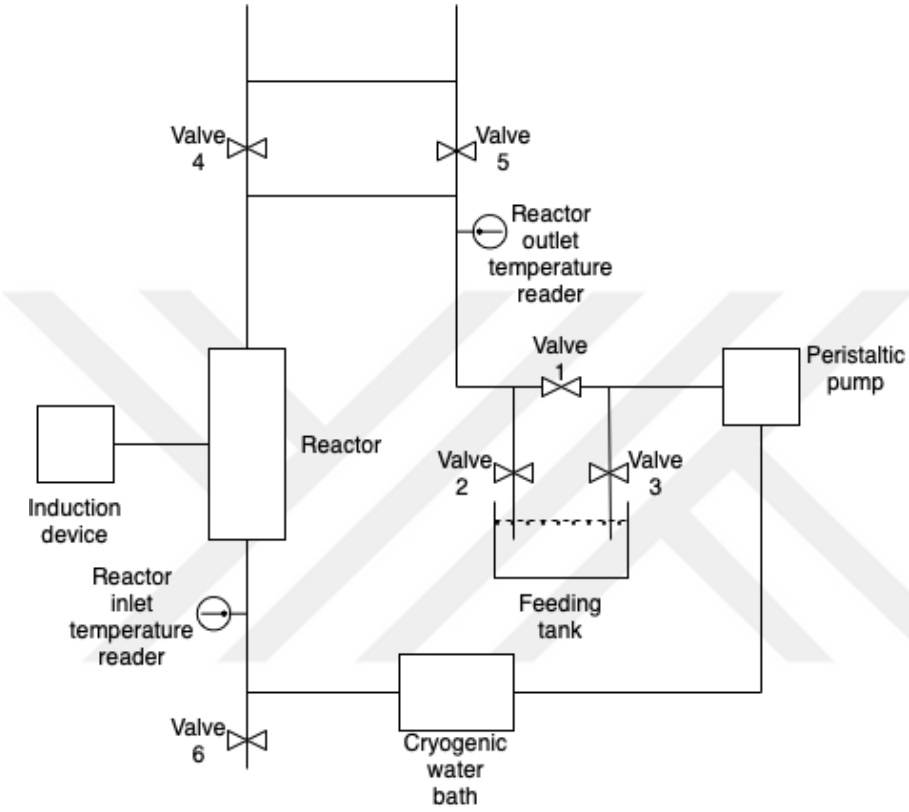

Figure 3.2 : Synthesis experiment setup

The induction device has an operating range between 2 kW and 5 kW and provides the heating of the cylindrical metal substrate placed in the reactor. The coil connected to the induction device is designed to surround the reactor. The reactor is made of teflon which can withstand the temperatures and corrosive environment required for the syntheses and is also transparent to induction. The peristaltic pump, which allows the synthesis mixture to be fed to the system and circulated throughout the experiment, has a flow range between 24 ml/min and 1994 ml/min. The cryostatic water bath is used for cooling the synthesis mixture heated in the reactor. The pipeline used in the experimental setup is made of silicone which can withstand the high alkalinity of the synthesis solution.

Before starting the synthesis experiments some preliminary preparations were made. Thermocouples used in the experiment were calibrated with the help of a calibrated thermometer and cryostatic water bath is adjusted to the desired temperature. After these preparations the clear synthesis solution was prepared.

Synthesis experiments were carried out using a clear solution with the composition of $50Na_2O$: $1Al_2O_3$: $5SiO_2$:$1000H_2O$. Sodium aluminate (molar composition: $1.249Na_2O$:Al_2O_3:$0.542H_2O$, Sigma Aldrich), sodium silicate (molar composition: $0.287Na_2O$:SiO_2:$8.0282H_2O$, Merck), sodium hydroxide (99% pure, Merck) and distilled water were used as the reactants.

For each synthesis experiment approximately 600 ml synthesis solution was prepared. A small part of the required amount of distilled water was separated into a beaker. This water was later used for rinsing remaining sodium silicate from the beaker. First, sodium hydroxide was added to the remaining distilled water and stirred with a magnetic stirrer for 10 minutes. After checking whether sodium hydroxide was dissolved properly, sodium aluminate was added and stirred for 5 minutes. After dissolving sodium aluminate, sodium silicate was added to the mixture and the beaker containing the sodium silicate was rinsed with previously separated distilled water. After mixing for another 5 minutes, magnetic stirrer was removed from the solution.

The prepared synthesis mixture was then fed to the system with the peristaltic pump. System was kept closed to the air at the beginning (valves 1, 4, 5 and 6 were closed, valves 2 and 3 were kept open). After the pipeline and reactor were completely filled with the synthesis mixture, the valves connected to the feeding tank (valves 2 and 3) were closed and valve 1 was opened to start the circulation of the reaction mixture in the system.

The solution passing through the pump enters the reactor and then passing through the cryogenic water bath returns to the pump and back to the reactor and so on, ensuring circulation. The temperature is monitored with the thermocouples located at the inlet and outlet of the reactor, and the system is waited to become stable. When the reactor inlet-outlet temperatures stabilize, the experiment is started by turning the induction device on. Induction coil surrounding the reactor creates an alternating magnetic field and this magnetic field heats the metal substrate. The reaction mixture, which passes through both inside and outside of the cylindrical metal substrate in the reactor, heats

up to some extent as a result of contact with the heated surfaces of the substrate before it exits the reactor, and then, while passing through the cryogenic water bath, it is cooled before it is fed back to the reactor again. During the experiment, the reactor inlet-outlet temperatures are monitored by thermocouples and kept at desired temperature values by adjusting the cryogenic water bath temperature and induction power.

After the experiment is carried out for the selected time at the desired parameters, the induction device is turned off and the system is allowed to cool down for 5 minutes. Then the peristaltic pump is turned off. Following another 5 minutes, the solution is slowly drained from the system using the drain valve (valve 6) in the system. Finally, the zeolite coated metal substrate removed from the reactor was rinsed by distilled water and kept in a controlled humidity environment.

3.3 Characterization Experiments

3.3.1 N_2 Permeation test

N_2 permeation through the zeolite-coated metal substrate was measured in a permeation system (Figure 3.3). The coated substrate was placed in a stainless-steel module and was fitted tightly at both ends with O-rings. The gas that has become saturated by passing through water was fed from the outside of the tubular substrate (retentate side) and the gas passing through the coating is collected at the inner side of the tubular substrate (permeable side). The flowrate of this permeate was measured with a soap bubble flowmeter. Pressure of the gas entering the module was also measured.

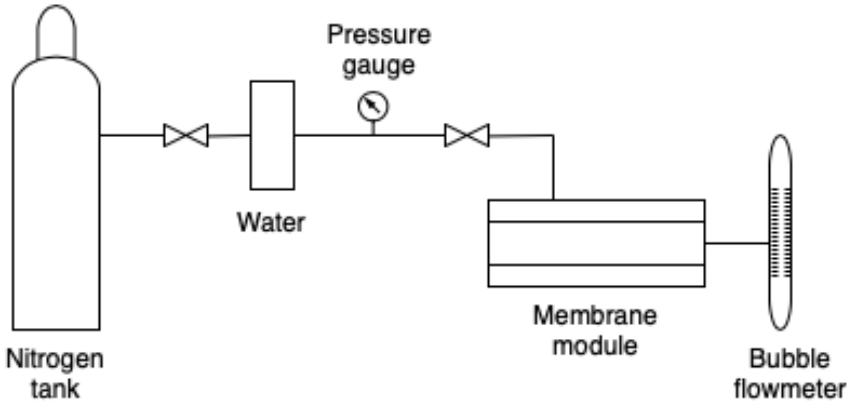

Figure 3.3 : N_2 permeation measurement test setup

With the assumption that the permeating gas is ideal, the permeance of the gas (mol/m^2.s.Pa) was calculated by the following equation,

$$Permeance = \frac{\frac{P}{RT}\frac{\Delta V}{\Delta t}}{\Delta P \cdot A} \quad (3.1)$$

where P is the atmospheric pressure (Pa), R is the ideal gas constant (Pa.m^3/K.mol), T is the room temperature (K), $\Delta V/\Delta t$ is the volumetric flow rate of the permeate (m^3/s) which is measured by the soap bubble flowmeter, ΔP is the transmembrane pressure difference (Pa) and A is the effective membrane area (m^2). In this study, the effective membrane area is the epoxy-free lateral area of the cylindrical substrate.

In the measurement system in our laboratory, permeance measurements can be made easily down to the level of 10^{-8} mol/m^2.s.Pa, but the system is not fit for measuring lower values clearly. For this reason, in this study, the expression $<10^{-9}$ was used for lower permeance values, which could not be measured accurately.

3.3.2 X-Ray diffraction analysis (XRD)

The samples taken from the coatings prepared on the substrates were characterized by XRD analyses in order to determine crystallinities and phase purities. When X-ray diffraction is applied, a distinctive diffraction pattern, which is like a fingerprint, is obtained for each crystal structure.

X-ray diffraction analyses were carried out with a PANanalytical X'Pert Pro model diffractometer using Cu $K\alpha_1$ radiation at 45 kV and 40 mA and data were collected over the range of 2Θ angles from 5° to 50° using 1°/min scan rate.

The strongest non-overlapping three peaks in the known diffraction patterns of zeolites are taken into the consideration when examining the analyses.

3.3.3 Thermogravimetric analysis (TGA)

The structure of zeolite A crystals are stable up to about 400 °C. On the contrary, amorphous structures are not stable and cannot remain intact at high temperatures. Since it is known that zeolite A maintains its crystallinity and thus its water adsorption capacity at 350 °C, TGA was applied to the same sample twice up to this temperature, consecutively in order to estimate the ratio of the crystalline material in the obtained solid, in other words, the crystallinity of the solid. If the weight loss in the second TGA

is much lower than the weight loss in the first TGA, this means that the solid contains a highly amorphous structure. If there is little or no difference between the weight loss in the second TGA and the weight loss in the first TGA, it can be said that the material contains a high percentage of crystals.

Thermogravimetric analysis (TGA) was performed with Perkin Elmer brand, Pyris Diamond TG-DTA model device. Before the TGA experiments, the samples were kept in a controlled humidity environment in order to ensure that the solid samples were saturated with moisture. After the first TGA, the same samples were kept in a controlled humidity environment for the second time, allowing them to reach moisture saturation again. A second TGA was applied to the saturated samples. In the TGA experiments, a program with a temperature range of 25 - 350 °C, a heating rate of 10 °C/min, and an isothermal step at 350 °C for 5 minutes was applied.

4. RESULTS AND DISCUSSION

4.1 Results of Calibration Experiments

Before starting the synthesis experiments, calibration experiments were carried out using water instead of synthesis solution for each substrate type. The purpose of these experiments was to determine the dependence of reactor inlet and outlet temperatures and thus the temperature difference obtained across the reactor on other system parameters, namely, the induction power, cryostatic water bath temperature and the flow rate. In each calibration experiment, induction power, cryostatic water bath temperature and flow rate were kept constant and the experiment was ended when the temperature values read by the thermocouples at the reactor inlet and outlet did not change any more. These inlet and outlet temperatures were noted. Later, the experimental parameters of the synthesis experiments to obtain the desired reactor inlet and outlet temperatures were chosen accordingly. Detailed results of these experiment are given in appendix A.

As a result of the calibration experiments, it was observed that the increase in the induction power increased the difference between the reactor inlet and outlet temperatures. In Figure 4.1, a graph showing the effect of different induction power values on the reactor inlet and outlet temperatures is given when the cryogenic water bath temperature is 5 ^{o}C and the flow rate is 149.6 ml/min (Substrate: 24x110/500). When the graph is examined, it is seen that the difference between the reactor inlet and outlet temperatures increases as the induction power increases.

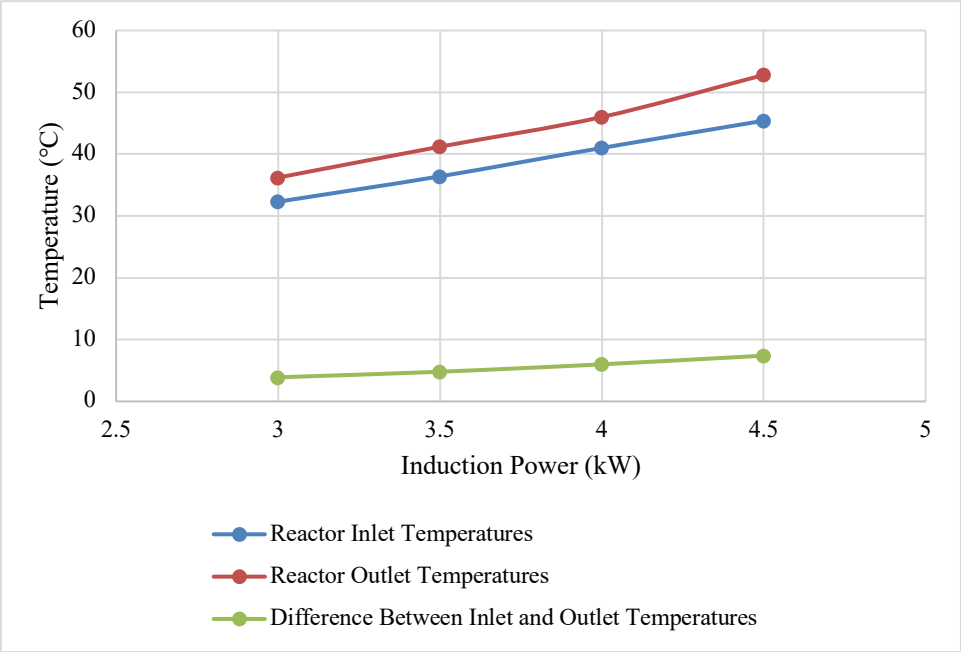

Figure 4.1 : Effect of induction power on system temperatures (cryogenic water bath temperature: 5 °C, flow rate: 149.6 ml/min, substrate: 24x110/500).

Another system variable is the cryogenic water bath temperature. Induction power and flow rate were kept constant to examine the effects of cryostat temperature on the system. It was observed that when the cryogenic water bath temperature increased, both the reactor inlet and outlet temperatures increased. The difference between the reactor inlet and outlet temperatures remained approximately constant. Figure 4.2 shows the effects of cryogenic water bath temperature on the system when the flow rate is 149.6 ml/min and the induction power is 4.5 kW (Substrate: 24x100/500/500).

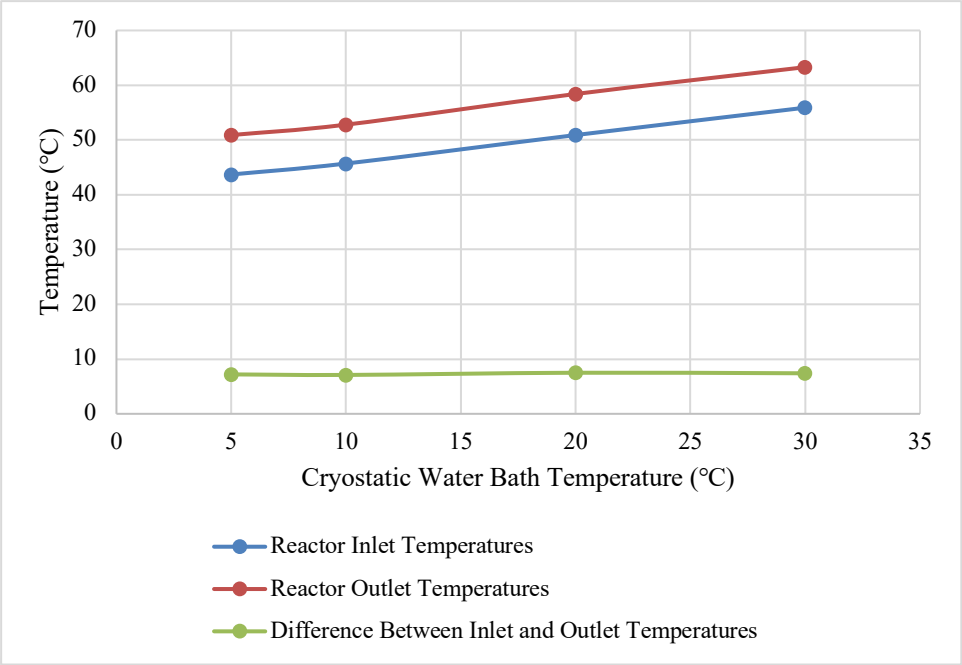

Figure 4.2 : Effect of cryostatic water bath temperature on system temperatures (induction power: 4.5 kW, flow rate: 149.6 ml/min, substrate: 24x110/500/500).

When the effects of flow rate on reactor inlet and outlet temperatures are examined, in cases where the induction power and cryostatic water temperature remained the same, it was observed that the inlet temperature increased with the increase in flow rate, but the outlet temperature decreased, in other words, the difference between the reactor inlet and outlet temperatures decreased. Figure 4.3 shows the effects of flow rate on temperatures when the induction power and cryostatic water bath temperature are kept the same.

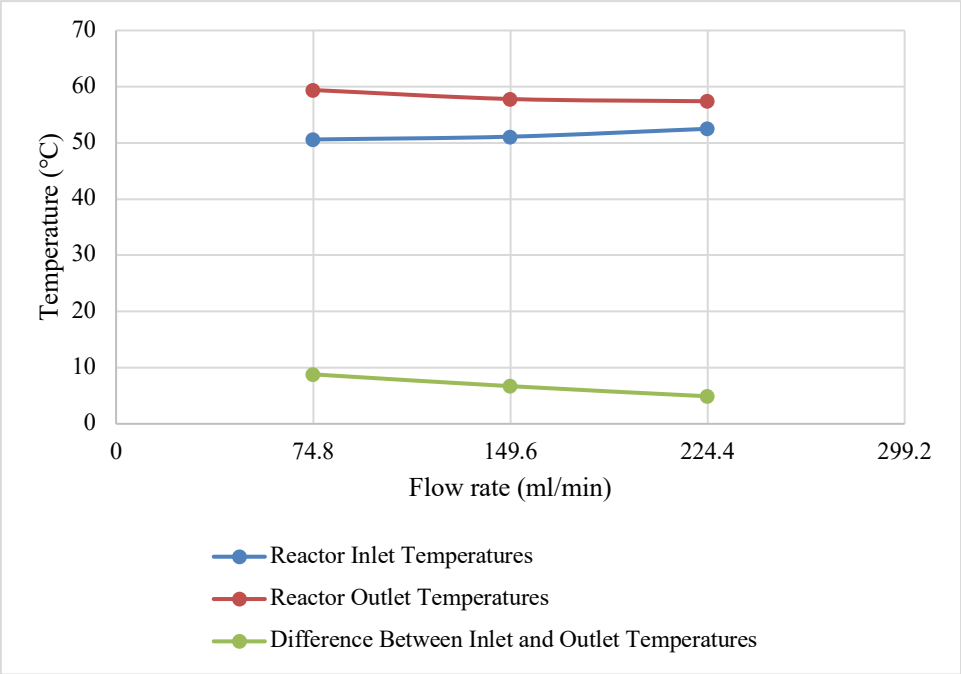

Figure 4.3 : Effect of flow rate on system temperatures (induction power: 4.0 kW, cryostatic water bath temperature: 20 °C, substrate: 24x110/200x1400).

When different types of metal substrates are used in the system, different experimental parameters had to be applied to find the same reactor inlet and outlet temperatures. Table 4.1 shows the effects of the different types of substrates used in this study, on the reactor inlet and outlet temperatures, keeping the flow rate, induction power and cryostatic water bath temperature constant at a set of chosen values.

Table 4.1 : Effect of different substrate types on system temperatures (induction power: 4.0 kW, flow rate: 149.6 mL/min, cryostatic water bath temperature: 20 °C).

Substrate type	Induction power (kW)	Flow rate (ml/min)	Cryostatic water bath temperature (°C)	Reactor inlet temperature (°C)	Reactor outlet temperature (°C)	Difference between inlet-outlet temperatures (°C)
24x110 /500	4.0	149.6	20	48.7	54.6	5.9
24x110 /500/500	4.0	149.6	20	46.4	52.1	5.7
24x110 /200x1400	4.0	149.6	20	51.1	57.8	6.7

4.2 Results of Zeolite A Coating Synthesis Experiments

4.2.1 Synthesis experiments with different types of substrates

Zeolite A coating synthesis experiments were started by testing two different substrate types. The first of these substrates was prepared with a single layer of 500 mesh sheet on a 24x110 micronic mesh sheet and the other one with two layers of 500 mesh sheets on a 24x110 micronic mesh sheet.

In order to test these substrate types with single layer 500 mesh sheet and double layer 500 mesh sheets on the outer side of the substrate, synthesis experiments were carried out for 1, 3 and 5 hours at 149.6 ml/min flow rate, and reactor inlet and outlet temperatures of 55 and 60 °C.

The conditions and results of the experiments performed for different synthesis times with 24x110/500 type substrate are given in Table 4.2.

Table 4.2 : Synthesis experiments using 24x110/500 substrate type.

	A1	A2	A3
Substrate Type	24x110/ 500	24x110/ 500	24x110/ 500
Power (kW)	2.2	2.2	2.0
Flow Rate (ml/min)	149.6	149.6	149.6
Water Bath Temperature (°C)	44.1	38.8	41.2
Inlet - Outlet Temperatures (°C)	55 - 60	55 - 60	55 - 60
Time (h)	1	3	5
Coating amount (g)	0.37	0.69	1.24
Coating thickness (μm)	49	92	164

As can be seen from the table, as the synthesis time increases, the amount, and thus the thickness of the coating increase.

Figure 4.4 and Figure 4.5 show the XRD results of the samples scraped from inner and outer surfaces of the coatings A2 and A3, together with that of commercial NaA, added for comparison.

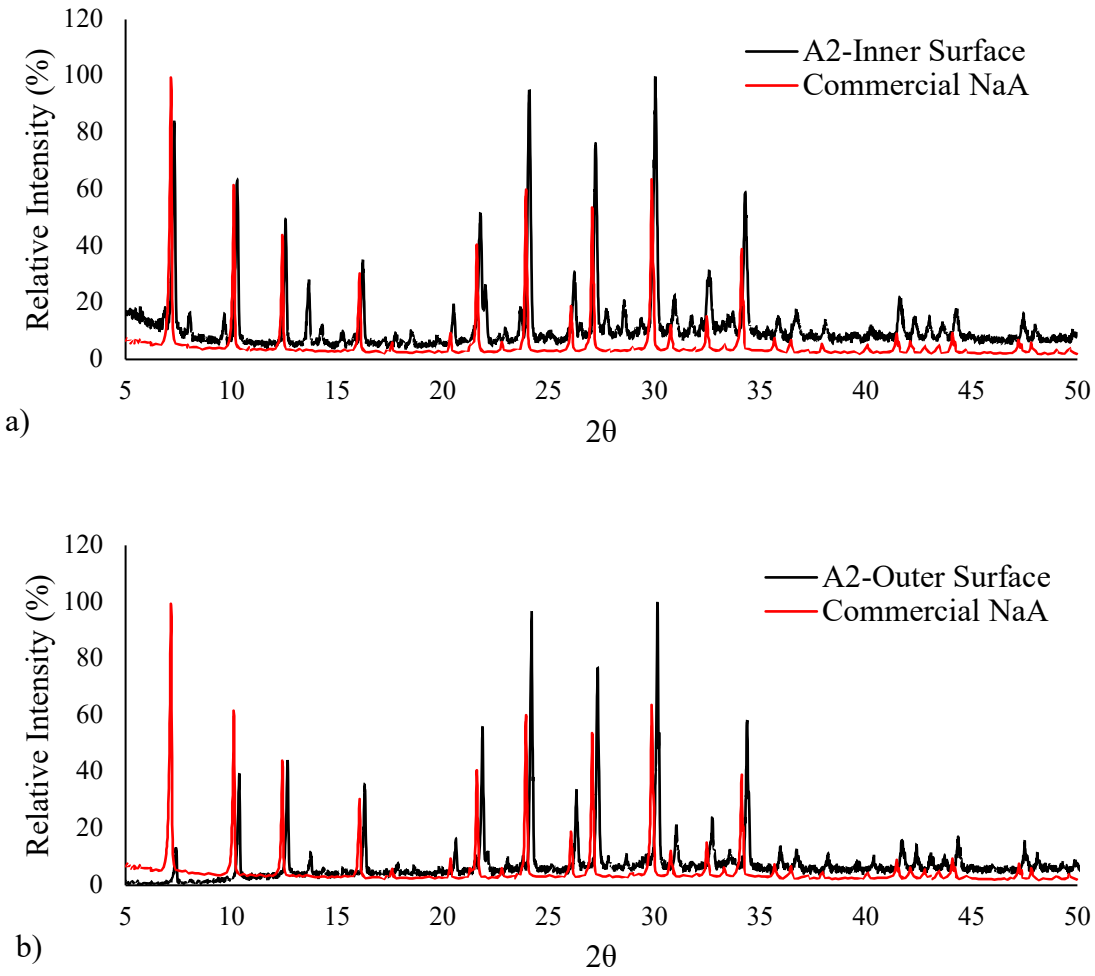

Figure 4.4 : Comparison of XRD results of the samples taken from the a) inner, and b) outer surface of the substrate coated in experiment A2, with that of commercial NaA

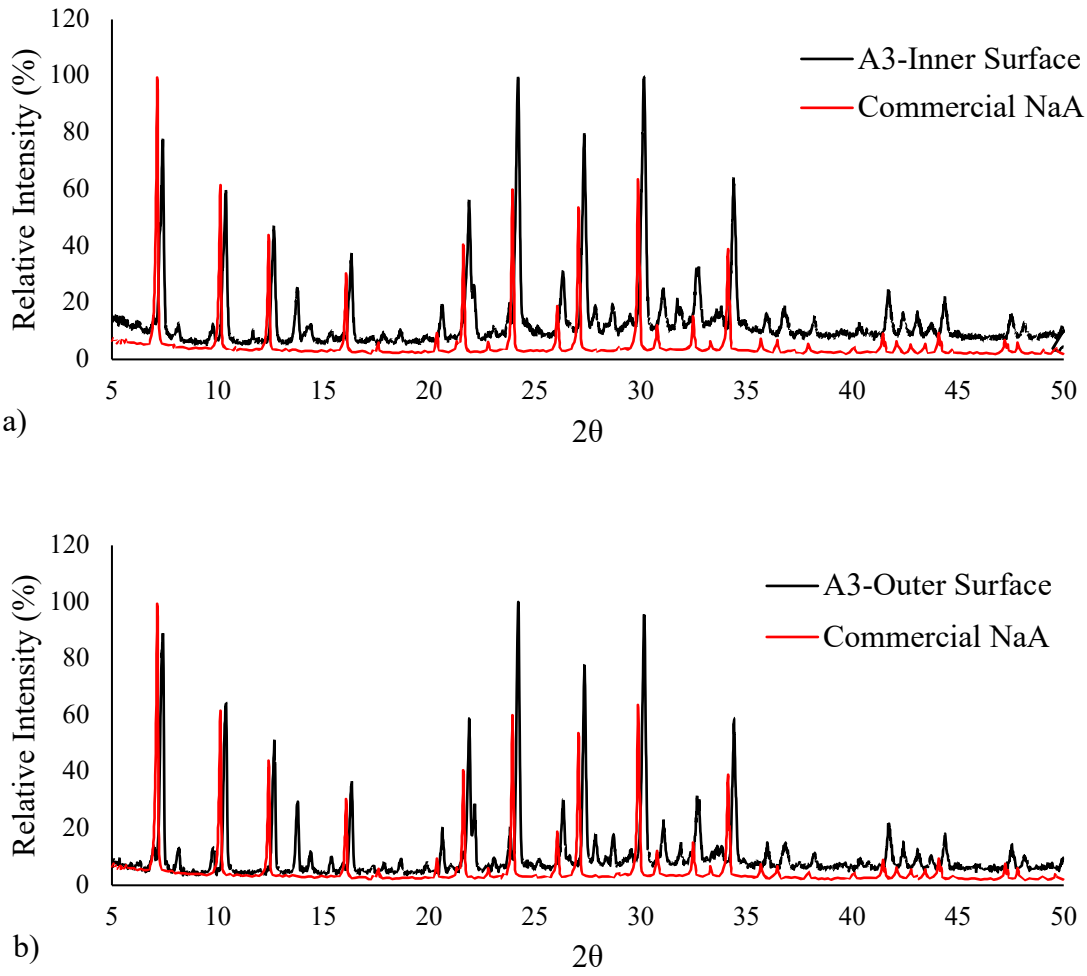

Figure 4.5 : Comparison of XRD results of the samples taken from the a) inner, and b) outer surface of the substrate coated in experiment A3, with that of commercial NaA

When the XRD results are examined, it is seen that the samples contain higher amounts of zeolite A (peak positions: 7.18°, 16.11°, 26.11°) in addition to lower amounts of zeolite LTN (peak positions: 6.77°, 7.94°, 13.56°) in some of them.

The LTN phase is a less studied phase compared to the LTA phase. It has one of the largest and most complex unit cells known. Like zeolite A, LTN is also synthesized at low temperatures, and transformation to sodalite is observed at high temperatures [39]. LTN has a 3-dimensional pore structure with 6 membered ring windows [2].

When the XRD results of the samples taken from the inner and outer surfaces of the coating A2, obtained after three hours of synthesis, are compared, it is seen that the LTN peaks in the XRD of the sample taken from the inner side are higher (Appendix B, Figure B.1.a). On the other hand, when the XRD graphs of the samples taken from the inner and outer surfaces of coating A3, obtained after 5 hours of synthesis, are

examined, no significant difference is observed between the samples (Appendix B, Figure B.1.b).

When the XRD results of the samples taken from the outer surfaces of the coated substrates obtained from these experiments were examined, it was seen that the LTN peaks in the XRD graph of A3 were higher, indicating that LTN formation increased with time on the outer surface (Appendix B, Figure B.2.a). LTN phase was not present at the earlier time on this side of the coating. There was no significant difference between the XRD graphs of the two samples obtained from the inner surfaces of A2 and A3 (Appendix B, Figure B.2.b). LTN peaks were present on both graphs, indicating that LTN has formed at an earlier time on this side of the substrate.

In order to compare the effect of the substrate type, synthesis experiments were also carried out using 24x110/500/500 type of substrate with similar experimental parameters as in the experiments with 24x110/500 substrate type. The conditions of these experiments and the results obtained are given in Table 4.3.

Table 4.3 : Synthesis experiments using 24x110/500/500 substrate type.

	A4	A5	A6
Substrate Type	24x110/ 500/500	24x110/ 500/500	24x110/ 500/500
Power (kW)	2.3	2.0	2.3
Flow Rate (ml/min)	149.6	149.6	149.6
Water Bath Temperature (°C)	38.3	53.4	40.4
Inlet - Outlet Temperatures (°C)	55-60	55-60	55-60
Time (h)	1	3	5
Coating Amount (g)	0.51	0.91	2.05
Coating Thickness (μm)	68	121	273

As can be seen from the table, similar to the experiments carried out using 24x110/500 substrate type, as the synthesis time increases, the amount of coating increases and accordingly, the coating thickens. Compared to the experiments carried out using 24x110/500 substrate type, in experiments carried out using 24x110/500/500 substrate type, coating amounts are higher and accordingly, coatings are thicker.

Figure 4.6 and Figure 4.7 show the XRD results of the samples scraped from inner and outer surfaces of the coatings A5 and A6, together with the XRD pattern of commercial NaA, added for comparison.

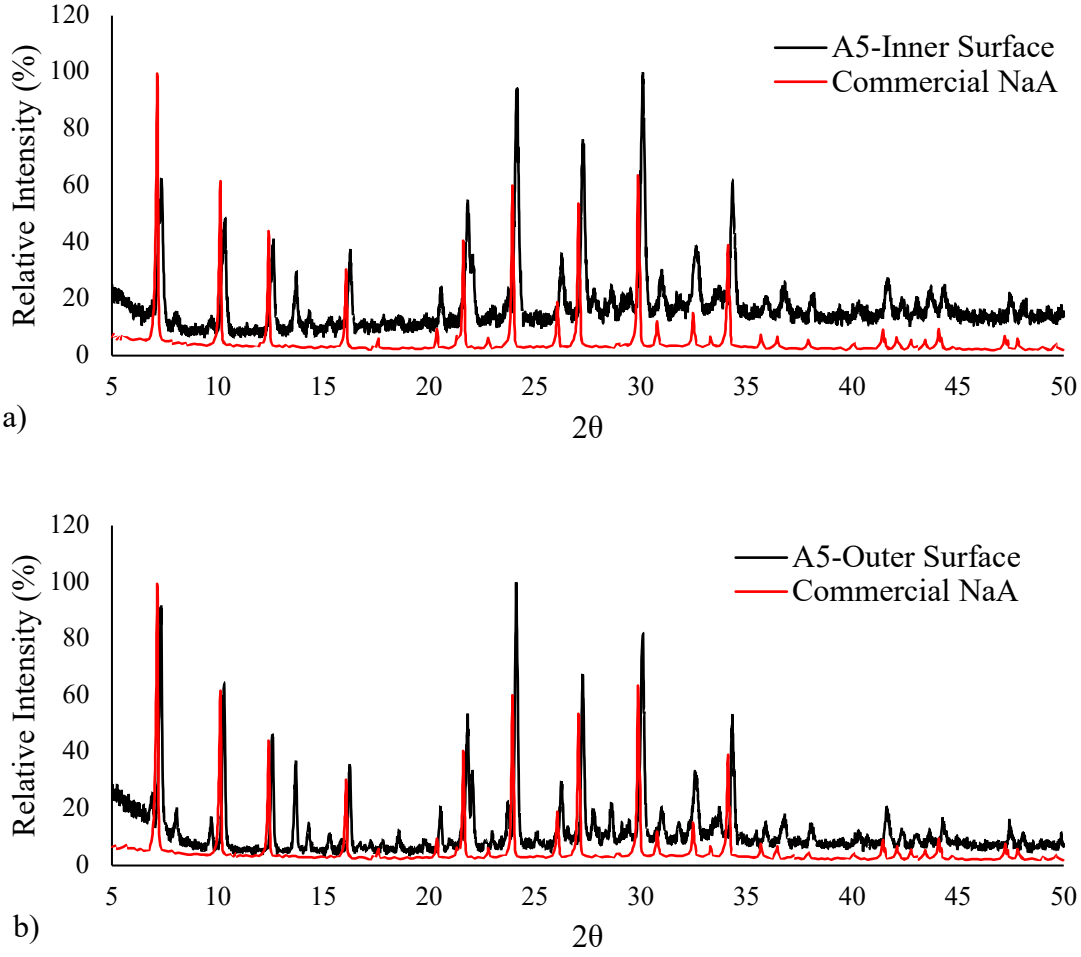

Figure 4.6 : Comparison of XRD results of the samples taken from the a) inner, and b) outer surface of the substrate coated in experiment A5, with that of commercial NaA

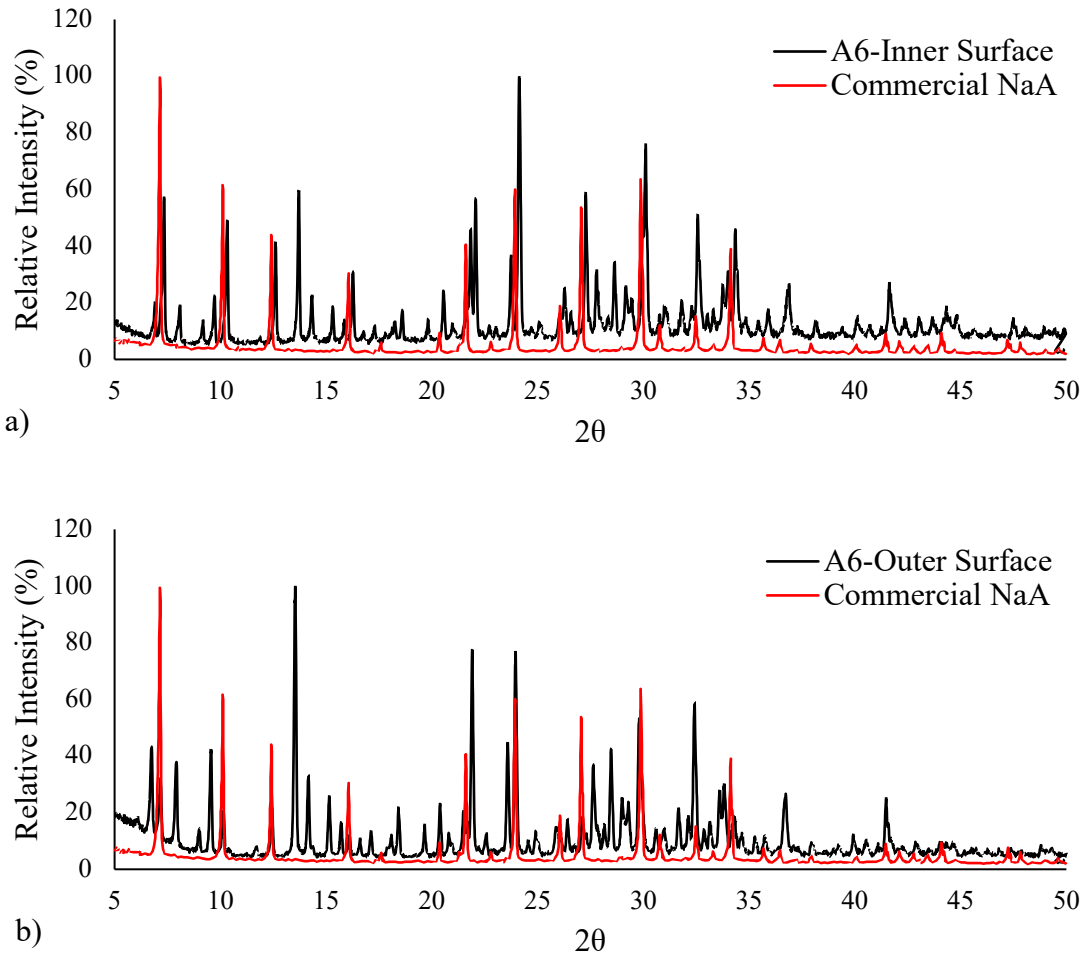

Figure 4.7 : Comparison of XRD results of the samples taken from the a) inner, and b) outer surface of the substrate coated in experiment A6, with that of commercial NaA

When the XRD results are examined, similar to the results of the experiments using supports prepared with a single layer of 500 mesh sheet on the outside, it is seen that the samples mainly contain zeolite A (peak positions: 7.18°, 16.11°, 26.11°) and zeolite LTN (peak positions: 6.77°, 7.94°, 13.56°). LTN peak intensities seem to be higher in the XRD patterns of the samples obtained from the coatings prepared on 24x110/500/500 substrate, when compared to those on 24x110/500 substrate.

When the XRD results of the samples taken from the inner and outer surfaces of A5, obtained after three hours of synthesis, are compared, no significant difference is observed between the samples (Appendix B, Figure B.3.a). On the other hand, when the XRD graphs of the samples taken from the inner and outer surfaces of A6, obtained after 5 hours of synthesis, are examined, it is seen that the LTN peaks in the XRD of

the sample taken from the outer layer seem to be somewhat higher (Appendix B, Figure B.3.b).

The peaks indicating the LTN phase in the samples taken from both the inner and outer surfaces of the coated substrate were observed to increase with time (Appendix B, Figure B.4). The increase was more pronounced on the outer surface of the coating. Intensities of the zeolite A peaks on the other hand, seemed to decrease with time, and the decrease was more pronounced on the outer surface of the coating. These results indicate that LTN phase increased with synthesis time at the expense of zeolite A.

When the substrates having single and double layers of 500 mesh sheets were compared, LTN peaks in the samples taken from the outer surfaces of the coatings were higher for the 24x110/500/500 substrate than for the 24x110/500 substrate. The differences were not pronounced when the samples taken from the inner surfaces were compared. Intensities of the LTN peaks were higher, while those of zeolite A peaks were lower for the coatings prepared on the 24x110/500/500 substrate, when compared to those on the 24x110/500 substrate. The differences were more pronounced for the samples taken from the outer surfaces of the coatings (Appendix B, Figure B.5 and Figure B.6).

Coated substrates with double layers of 500 mesh sheets on the outside (24x110/500/500) were cut and examined visually too. It was observed that a thin layer of coating has also formed between the two layers of 500 mesh sheets, albeit a small amount. Thin layers of coating were also observed to have formed between the 24x110 and the 500 mesh layer(s) for the substrates. The corresponding amount for the substrates with single layer of 500 mesh sheets on the outside was higher.

As was mentioned above, the coatings obtained in the experiments using 24x110/500/500 substrate type were thicker. The coatings prepared on this type of substrate also contained higher amounts of LTN phase when compared to the coatings on the 24x110/500 substrate. In the light of these results, 24x110/500 substrate with a single outer layer of 500 mesh sheet was chosen as more suitable to be used for the preparation of relatively thin zeolite A coatings.

After deciding on the use of a single outer layer, another type of substrate having a micronic mesh sheet of 200x1400 on the outside, was developed. This 200x1400

micronic mesh sheet has 10 μm openings, smaller than those of the 500 mesh sheet, which has 25 μm openings between its wires.

At this stage, with a few upgrades in the welding process, improved substrates, in terms of figural smoothness, started to be manufactured and used. In this way, it has become possible to test the coatings prepared on the selected substrates with gas permeance measurements. N_2 permeance measurements were carried out to test how continuous and closed the prepared coatings were.

To test the possibility of obtaining a thinner and closed layer of zeolite coating using N_2 permeance measurements, the reactor inlet and outlet temperatures were decreased from 55 and 60 °C to 45 and 50°C. The flow rate was kept at the same value of 149.6 ml/min as in previous experiments. 24x110/500 and 24x110/200x1400 substrate types were used, and 1, 2, 3 and 5 hours of synthesis experiments were carried out. The results are given in Tables 4.4 and 4.5, for the substrate types 24x110/500 and 24x110/200x1400, respectively.

Table 4.4 : Synthesis experiments using 24x110/500 substrate type.

	A7	A8	A9	A10
Substrate Type	24x110/ 500	24x110/ 500	24x110/ 500	24x110/ 500
Power (kW)	4.0	4.1	4.0	4.2
Flow Rate (ml/min)	149.6	149.6	149.6	149.6
Water Bath Temperature (°C)	10.9	14.7	11.7	13.0
Inlet - Outlet Temperatures (°C)	45-50	45-50	45-50	45-50
Time (h)	1	2	3	5
Coating Amount (g)	0.28	0.60	0.85	0.97
Coating Thickness (μm)	37	79	112	128
N_2 Permeance (mol/m^2.s.Pa)	1.34×10^{-3}	6.00×10^{-4}	1.19×10^{-4}	7.57×10^{-5}

Table 4.5 : Synthesis experiments using 24x110/200x1400 substrate type.

	A11	A12	A13	A14
Substrate Type	24x110/ 200x1400	24x110/ 200x1400	24x110/ 200x1400	24x110/ 200x1400
Power (kW)	3.8	3.6	3.4	3.8
Flow Rate (ml/min)	149.6	149.6	149.6	149.6
Water Bath Temperature (°C)	11.2	12.9	13.3	11.6
Inlet - Outlet Temperatures (°C)	45-50	45-50	45-50	45-50
Time (h)	1	2	3	5
Coating Amount (g)	0.35	0.47	0.79	1.11
Coating Thickness (μm)	46	62	104	146
N_2 Permeance (mol/m^2.s.Pa)	1.76×10^{-4}	4.30×10^{-4}	5.52×10^{-5}	2.82×10^{-5}

As can be seen from the Tables 4.4 and 4.5, there is no obvious difference between the coating thicknesses obtained with the two substrate types. However, it is seen that the coatings prepared on the 24x110/200x1400 substrate type gave slightly smaller gas permeance values, indicating that the coatings obtained with this substrate were more closed. For this reason, the zeolite A coating experiments were continued in this study using 24x110/200x1400 substrates.

4.2.2 Synthesis experiments at different flow rates

As known from the results of calibration experiments, when the flow rate increases and the contact time of the synthesis solution with the substrate decreases, more induction power is required to obtain the same reactor inlet and outlet temperatures. Inversely, less induction power is required when operating at a lower flow rate. Induction power is important since it also influences the surface temperature on the substrate. Surface temperature is different than the temperature in the synthesis solution, and it also influences the quality of the coating. In order to examine the effect of different flow rates and to choose a suitable flow rate for further experiments, three flow rates were selected, 74.8, 149.6 and 224.4 ml/min. With these three selected flow rates, synthesis experiments were carried out for 3 hours, at the reactor inlet and outlet temperatures of 45 and 50°C. The results of these experiments are given in Table 4.6.

Table 4.6 : Synthesis experiments at different flow rates.

	A15	A13	A16
Substrate Type	24x110/200x1400	24x110/200x1400	24x110/200x1400
Power (kW)	4.1	3.4	2.8
Flow Rate (ml/min)	224.4	149.6	74.8
Water Bath Temperature (°C)	1.6	13.3	32
Inlet - Outlet Temperatures (°C)	45-50	45-50	45-50
Time (h)	3	3	3
Coating Amount (g)	1.05	0.79	0.44
Coating Thickness (µm)	139	104	58
N_2 Permeance (mol/m^2.s.Pa)	7.71×10^{-5}	5.52×10^{-5}	7.81×10^{-6}

The results of these experiments performed at different flow rates, make it clear that the right choice for preparing thinner and closed coatings is using lower flow rate. In the experiment performed at 224.4 ml/min, 1.05 g amount of coating was obtained, while 0.79 g of coating was obtained from the experiment performed at 149.6 ml/min

flow rate. Both coatings had N_2 permeance values on the order of 10^{-5} mol/m^2.s.Pa; the latter had a slightly smaller permeance. The experiment performed at the lowest flow rate of 74.8 ml/min, gave the smallest coating amount, 0.44 g, and lowest N_2 permeance, which was on the order of 10^{-6} mol/m^2.s.Pa.

The decrease in the induction power requirement of the system together with the decreasing flow rate resulted in reducing the amount of coating. As the induction power applied to the metal substrate decreases, the surface temperature of the metal also decreases. As a result of the decrease in the surface temperature of the substrate, rates of the processes, such as nucleation and crystal growth taking place on the substrate surface during zeolite synthesis, will also slow down. Lower flow rate in the solution, resulting in lower crystallization rates on the surface, understandably resulted in the preparation of thinner and more closed coatings.

4.2.3 Synthesis experiments at different inlet - outlet temperatures

Zeolite synthesis is basically a crystallization reaction and has an exponential dependence on temperature. In the induction heating system, crystallization takes place in a thermal boundary layer on the substrate and hence is affected not only by the surface temperature of the substrate, but also by the temperature of the synthesis solution flowing over the substrate. With the increase in temperature, the formation of nuclei and the growth of these nuclei accelerate, and with the decrease in temperature, the formation of nuclei and the growth of nuclei slow down. Both lowering and raising the temperature have their advantages. It may be expected that the coating thickness will decrease as the temperature decreases, since the activation energy of crystal growth is larger than that of nucleation for zeolite synthesis. On the other hand, the obtained coating may not be fully crystalline and may contain amorphous structures, since crystallization will slow down at lower temperatures. There is also a possibility that the holes of the mesh sheets may not be fully closed by zeolite crystals, at coating thickness values lower than a threshold value. The gas permeance will likely be higher than the permeance of the zeolite micropores in these cases. As the temperature rises, on the other hand, the thickness of the coating will increase while the resulting coating is also expected to be more crystalline compared to coatings prepared at lower temperatures. Although the gas permeance of a thicker and more crystalline coating is expected to be lower, there is also the possibility of the presence of larger mesopores

being left between the crystals, as a result of the rapid growth on the substrate, leading to the formation of an irregular zeolite crystal layer.

A series of experiments with different reactor inlet and outlet temperatures were thus planned and carried out in order to investigate the effects of these temperatures on the coating properties, and to optimize their values. Synthesis experiments for 3 hours at 74.8 ml/min flow rate at different reactor inlet and outlet temperatures from 35 and 40 °C to 55 and 60 °C were performed using 24x110/200x1400 substrate type. The conditions and results of these experiments are given in Table 4.7.

Table 4.7 : Synthesis experiments at different reactor inlet-outlet temperatures (Synthesis time: 3 hours).

	A17	A18	A19	A20	A21
Substrate Type	24x110/ 200x1400	24x110/ 200x1400	24x110/ 200x1400	24x110/ 200x1400	24x110/ 200x1400
Power (kW)	2.6	2.6	2.8	2.8	2.7
Flow Rate (ml/min)	74.8	74.8	74.8	74.8	74.8
Water Bath Temperature (°C)	14	25	28	33	41
Inlet - Outlet Temperatures (°C)	35-40	40-45	45-50	50-55	55-60
Time (h)	3	3	3	3	3
Coating Amount (g)	0.21	0.42	0.87	1.40	1.89
Coating Thickness (μm)	28	56	116	186	252
N_2 Permeance (mol/m^2.s.Pa)	1.70×10^{-3}	2.60×10^{-6}	8.91×10^{-6}	7.70×10^{-5}	8.40×10^{-4}

As seen from the experimental results, the coating thickness increased with the increase in reactor inlet and outlet temperatures. The gas permeance, however, seemed to decrease with the increase in coating thickness at low thickness values, while it started to increase again above coating thickness values of about 100 μm. Thus, thinner and more continuous and compact coatings were obtained for coating thickness values of about 100 μm under these experimental conditions. N_2 permeance values on the order of 10^{-6} mol/m^2.s.Pa, on the other hand, are still considered to be higher than the values expected ($<10^{-9}$ mol/m^2.s.Pa) for a continuous and relatively defect-free zeolite coating. Another series of experiments was therefore planned to examine the variation of the thickness and permeance of the zeolite coatings with temperature, synthesized at a longer time of 5 hours synthesis. Since the coatings were expected to grow more at this longer time, lower inlet and outlet temperatures to and from the reactor of 30-

35 °C were also included, and those of 55-60 °C were excluded in the investigation. The conditions and results of these experiments are given in Table 4.8.

Table 4.8 : Synthesis experiments at different reactor inlet and outlet temperatures (Synthesis time: 5 hours)

	A22	A23	A24	A25	A26
Substrate Type	24x110/ 200x1400	24x110/ 200x1400	24x110/ 200x1400	24x110/ 200x1400	24x110/ 200x1400
Power (kW)	2.5	2.6	2.6	2.8	2.8
Flow Rate (ml/min)	74.8	74.8	74.8	74.8	74.8
Water Bath Temperature (°C)	5	14	25	28	33
Inlet - Outlet Temperatures (°C)	30-35	35-40	40-45	45-50	50-55
Time (h)	5	5	5	5	5
Coating Amount (g)	0.35	0.54	0.87	1.24	1.92
Coating Thickness (μm)	47	72	116	165	256
N_2 Permeance (mol/m^2.s.Pa)	1.01×10^{-4}	1.12×10^{-6}	5.78×10^{-6}	3.30×10^{-5}	2.24×10^{-3}

As can be seen from the results, the coating thickness increased with the increase in reactor inlet and outlet temperatures as expected. Similar to the results of the experiments carried out at 3 hours of synthesis, there seemed to be an optimum thickness value around 100 μm, regarding the gas permeance values obtained. When the experiments performed at reactor inlet-outlet temperatures of 35-40 °C at different synthesis times are compared, it is seen that the prolongation of the synthesis time from 3 hours to 5 hours decreases the gas permeance. In the experiments carried out at 45-50 and 50-55 °C of reactor inlet-outlet temperatures, it was observed that the gas permeance increased with the increase in synthesis time from 3 hours to 5 hours.

The result of these experiments carried out at different reactor inlet and outlet temperatures and at different synthesis times show once more that for the preparation of a thin and relatively defect-free coating, the synthesis time and reactor inlet-outlet temperatures must be chosen carefully.

4.2.4 Multiple staged synthesis experiments

In order to obtain a relatively defect-free thin zeolite coating on the selected metal mesh substrate, in the first stage, it is necessary to ensure uniform nucleation on the metal wires in the metal mesh sheets of the substrate, and then to grow the zeolite

crystals on this mesh sheet in a controlled manner to close the openings between the metal wires to obtain a crystalline zeolite layer.

With this approach, it was thought that it could be tried to run the experiment in stages with different reactor inlet-outlet temperatures. In the first stage of the experiment, it was aimed to facilitate nucleation slowly with lower reactor inlet-outlet temperatures, and then to accelerate the crystallization in the second stage by increasing the reactor inlet-outlet temperatures. In this direction, a number of experiments including different combinations of temperatures and synthesis times were tried.

First, to see if this two-staged experiment idea would be useful, two experiments were conducted. These experiments consisted of a 3 hours of first stage at reactor inlet-outlet temperatures of 45-50°C, followed by a 1 or 2 hours of second stage at reactor inlet-outlet temperatures of 55-60 °C. In order to be able to evaluate the results of these experiments, the results of the experiment conducted at reactor inlet-outlet temperatures of 45-50 °C for 3 hours without a second stage are also given in Table 4.9, for comparison.

Table 4.9 : Two staged synthesis experiments with different duration of second stage.

	A16	A27	A28
Substrate Type	24x110/ 200x1400	24x110/ 200x1400	24x110/ 200x1400
Power (kW)	2.8	2.8	2.5
Flow Rate (ml/min)	74.8	74.8	74.8
Water Bath Temperature (°C)	32	30-40	36-46
Inlet - Outlet Temperatures (°C)	45-50	45-50 55-60	45-50 55-60
Time (h)	3	3 + 1	3 + 2
Coating Amount (g)	0.44	0.93	1.59
Coating Thickness (µm)	58	123	210
N_2 Permeance (mol/m^2.s.Pa)	7.81×10^{-6}	6.84×10^{-9}	$<10^{-9}$

As can be seen from the table, when experiments A16 and A27 are examined, it can be noticed that even raising the reactor inlet-outlet temperatures by 10 °C and continuing the experiment for 1 more hour reduced the gas permeance from a value on the order of 10^{-6} to a value on the order of 10^{-9}. When the second stage is prolonged to two hours, no gas permeance in the system could be observed. Since the lowest gas permeance value that can be measured in the system used was on the order of 10^{-9}, the

gas permeance measurement results that were too low to be measured were indicated as $<10^{-9}$. With the second stage added, in addition to the decrease in gas permeance, the amount of coating also increased. The coating amount and hence the thickness almost doubled in the second stage for the experiment A27. The smallest thickness obtained was 210 μm for the only coating synthesized so far in this study (A28) with a gas permeance value lower than 10^{-9} mol/m^2.s.Pa.

As mentioned previously, the thickness values reported in the study are mass equivalent thickness values calculated for corresponding compact zeolite coatings of equal mass on the lateral curved surfaces of tubular supports of same diameter. These values, therefore, do not correspond to actual thickness values. They are only used as indicators to optimize the synthesis conditions to prepare thinner coatings with lower permeabilities. The actual effective thickness value of the coating across which gas permeation takes place is expected to be lower than the equivalent thickness value for the substrates used in this study.

In order to decrease the equivalent thickness value, two staged synthesis approach was further investigated by keeping one of the first or second stages same and changing the reactor inlet-outlet temperatures of the other stage. First, three experiments were carried out with first stages being similar with reactor inlet-outlet temperatures being kept at the lower values of 40-45 °C this time, for a synthesis time of 3 hours. The second stages of these experiments were carried out for 2 hours at reactor inlet-outlet temperatures of 45-50, 50-55 and 55-60 °C. The results of these experiments are given in Table 4.10.

Table 4.10 : Two staged synthesis experiments with second stages at different temperatures.

	A31	A29	A30
Substrate Type	24x110/ 200x1400	24x110/ 200x1400	24x110/ 200x1400
Power (kW)	2.2	2.1	2.1
Flow Rate (ml/min)	74.8	74.8	74.8
Water Bath Temperature (°C)	37-56	33-45	29-41
Inlet - Outlet Temperatures (°C)	40-45 55-60	40-45 50-55	40-45 45-50
Time (h)	3 + 2	3 + 2	3 + 2
Coating Amount (g)	1.36	0.91	0.71
Coating Thickness (μm)	181	121	94
N_2 Permeance(mol/m^2.s.Pa)	4.89×10^{-8}	5.74×10^{-8}	3.28×10^{-7}

The equivalent thickness and permeance values obtained after 3 h at reactor inlet-outlet temperatures of 40-45 °C was 56 μm and $2.60x10^{-6}$ mol/m^2.s.Pa (Table 4.7). As can be seen from Table 4.10, the change in reactor inlet-outlet temperature in the second stage affected the coating thickness more significantly, while it affected the gas permeance less. Considering the results of experiment A30 conducted at a lower second stage temperature, it is seen that the time is not sufficient. Considering the experiments A31 and A29, there is a clear increase in the coating thickness with the increase in temperature, while the gas permeance results are very close to each other.

At the end of these two-stage experiments, in order to reduce the gas permeance of the coating further, an additional healing step was applied using newly prepared synthesis solution. It is to be able to reduce the defects on the coating with a short synthesis experiment carried out at lower reactor inlet and outlet temperatures. For this purpose, the experiments A29 and A30 which yielded thinner coatings were chosen. Synthesis experiments were carried out for 2 hours at the temperatures of 45-50 applied in the first stage of their synthesis. Results of these experiments are given in Table 4.11.

Table 4.11 : Synthesis experiments with healing steps.

	A29	A29-2	A30	A30-2
Substrate Type	24x110/ 200x1400	24x110/ 200x1400	24x110/ 200x1400	24x110/ 200x1400
Power (kW)	2.1	2.2	2.1	2.2
Flow Rate (ml/min)	74.8	74.8	74.8	74.8
Water Bath Temperature (°C)	33-45	36	29-41	32
Inlet - Outlet Temperatures (°C)	40-45 50-55	40-45	40-45 45-50	40-45
Time (h)	3 + 2	2	3 + 2	2
Coating Amount (g)	0.91	1.70	0.71	1.14
Coating Thickness (μm)	121	226	94	152
N_2 Permeance (mol/m^2.s.Pa)	$5.74x10^{-8}$	$<10^{-9}$	$3.28x10^{-7}$	$<10^{-9}$

As can be seen from the table, healing step seems to work quite well in decreasing the gas permeance of coatings. But on the other hand, at the end of the healing step, the coating thickness almost doubled in both experiments. Still, the coating denoted A-30-2 had a lower thickness of 152 μm than that of the coating A-28, which was 210 μm. In the healing experiment, the existing zeolite coating may have provided a kind of seeding effect, causing the synthesis to progress very quickly. Although the gas

permeance decreases with healing steps, the increase in the coating thickness reduces the usability of this method. Healing steps using fresh reaction mixtures can be applied after single stage synthesis, for shorter synthesis times, at lower reactor inlet and outlet temperatures and for thinner coatings.

In order to understand the effect of changing the reactor inlet-outlet temperatures of the first stage, two more experiments were planned and carried out in addition to experiment A29. The second stages were kept the same and the temperature values of the first stages were changed. The second stages of these experiments had 2 hours of synthesis time at reactor inlet-outlet temperatures of 50-55 °C, as in the experiment A29. The first stages of these experiments had 3 hours of synthesis time at reactor inlet-outlet temperatures of 35-40, 40-45 and 45-50 °C, when experiment A29 was included. The results of these experiments are compared in Table 4.12.

Table 4.12 : Two staged synthesis experiments with different first stages.

	A32	A29	A33
Substrate Type	24x110/ 200x1400	24x110/ 200x1400	24x110/ 200x1400
Power (kW)	2.3	2.1	2.2
Flow Rate (ml/min)	74.8	74.8	74.8
Water Bath Temperature (°C)	29-47	33-45	36-43
Inlet - Outlet Temperatures (°C)	35-40 50-55	40-45 50-55	45-50 50-55
Time (h)	3 + 2	3 + 2	3 + 2
Coating Amount (g)	1.12	0.91	0.85
Coating Thickness (µm)	149	121	112
N_2 Permeance (mol/m^2.s.Pa)	3.91×10^{-6}	5.74×10^{-8}	$<10^{-9}$

When Table 4.12 is examined, it can be seen that the effect of the temperature change of the first stage against the temperature changes of the second stage is more striking. As the temperature of the first stage increased in the range tested in these experiments, both the coating thickness and the gas permeance values decreased.

The coating obtained with the experiment A33 was observed to have a sufficiently low gas permeance value (lower than 10^{-9} mol/m^2.s.Pa), as was obtained for A28, with almost half the equivalent thickness value obtained for the coating A28. The thickness obtained was 210 µm for the coating A28, while it was 112 µm for A33.

Figure 4.8 shows the XRD results of the samples scraped from outer surface of the coatings A28 and A33, together with the XRD pattern of commercial NaA, added for comparison.

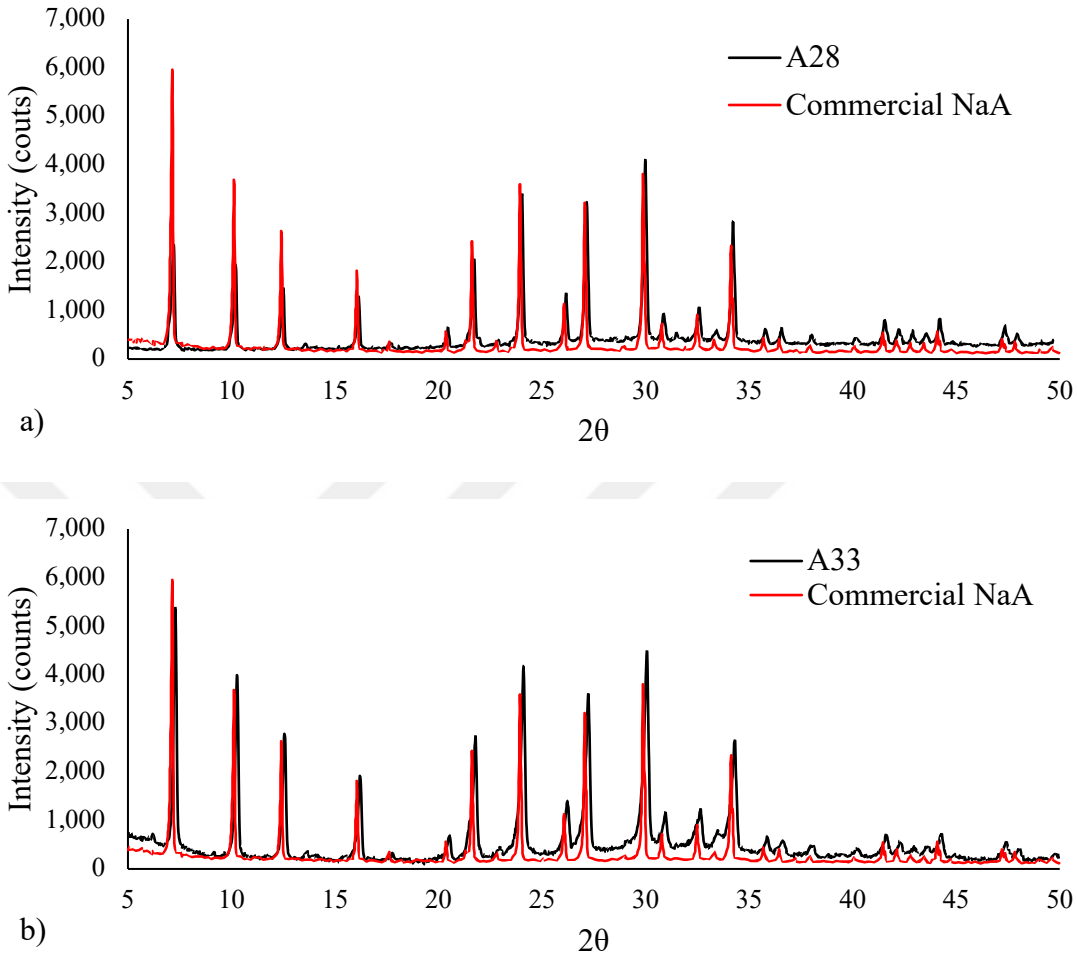

Figure 4.8 : Comparison of XRD results of the samples taken from the outer surface of the substrates coated in a) experiment A28, and b) A33, with that of commercial NaA

When the XRD results are examined, it is seen that the samples contain zeolite A (peak positions: 7.18°, 16.11°, 26.11°) and they are highly crystalline. For the sample taken from A28, two very small extra peaks are noticed at positions 13° and 32°. For the sample taken from A33, extra peaks are seen at positions 4°, 9° and 13°, but these peaks are also observed to be quite small.

In addition, TGA is conducted to the sample obtained from experiment A33. 1. TGA and 2. TGA are resulted in 18.8% and 18.5%, respectively. It is known that the zeolite A has 18% of adsorption capacity. With these results it can be confirmed that the

sample contains high amounts of zeolite A and the very small difference between the two TGA results confirms that the sample is highly crystalline.

5. CONCLUSIONS AND RECOMMENDATIONS

Applicability of the induction heating method to the preparation of zeolite A coatings on cylindrical metal substrates that may be suitable for use in separation applications was tested in this study. The effects of substrate type and system/synthesis parameters on the properties and performance of the synthesized zeolite A coating were examined.

Three types of metal substrates were developed to be used in this study. A thicker and more rigid 24x110 micronic mesh sheet was used on the inner surface of all three substrates. As the outer layer, single layer 500 mesh, double layer 500 mesh and single layer 200x1400 micronic meshes were used. 500 mesh sheet has 25 μm openings between its wires and 200x1400 micronic mesh sheet has 10 μm openings.

The dependence of reactor inlet and outlet temperatures and thus the temperature difference obtained across the reactor on other system parameters could be determined with the help of calibration experiments carried out using water instead of synthesis solution, before the synthesis experiments.

An additional zeolite phase besides LTA, the LTN phase, was seen to be present in smaller amounts, in the coatings prepared as a result of the initial experiments carried out on the substrate types, 24x110/500 (single outer layer), and 24x100/500/500 (double outer layers). The substrate with the single outer layer (24x110/500) was chosen to be more preferable, both due to the lower thickness values obtained for the coatings, and due to lower amounts of LTN phase present in the coatings prepared on this substrate.

Among the substrates with single outer layers, 24x110/500 and 24x110/200x1400, the latter was observed as the more preferable substrate type to be used in further studies due to the lower gas permeance and equivalent thicknesses values obtained for the coatings prepared on it. For this reason, zeolite A coating experiments were continued using 24x110/200x1400 substrates.

The effect of flow rate on the properties of the coatings prepared were investigated in order to choose a suitable flow rate for further experiments. It was observed that

thinner and more closed coatings could be obtained using lower flow rates. Lower flow rate in the solution, resulting in lower crystallization rates on the surface, understandably resulted in the preparation of thinner and more closed coatings.

Synthesis experiments were performed for investigation the effects of different reactor inlet and outlet temperatures on the coating properties. The coating thickness increased with the increase in reactor inlet and outlet temperatures. The gas permeance, however, seemed to decrease with the increase in coating thickness at low thickness values, while it started to increase again above coating thickness values of about 100 μm.

In order to optimize the effects of reactor inlet-outlet temperatures to prepare thinner coatings with lower permeabilities, the experiments were carried out with multiple stages with different reactor inlet-outlet temperatures. The two-staged experiments consisted of a first stage at lower reactor inlet-outlet temperatures, followed by a second stage at slightly higher reactor inlet-outlet temperatures. This approach was shown to be successful in obtaining coatings with lower permeabilities.

The smallest equivalent thickness obtained with the above approach was 210 μm for the only coating synthesized with a gas permeance value lower than 10^{-9} mol/m^2.s.Pa, in these initial two staged experiments. This coating was obtained with 3 hours of first stage at reactor inlet-outlet temperatures of 45-50°C, followed by 2 hours of second stage at reactor inlet-outlet temperatures of 55-60 °C.

Two staged synthesis approach was further investigated by keeping one of the first or second stages same and changing the reactor inlet-outlet temperatures of the other stage. The change in reactor inlet-outlet temperature in the second stage affected the coating thickness more significantly, while it affected the gas permeance less. The effect of the temperature change of the first stage against the temperature changes of the second stage was observed to be more striking. As the temperature of the first stage increased in the range tested in these experiments, both the equivalent coating thickness and the gas permeance values decreased.

The coating obtained from the experiment with the reactor inlet-outlet temperatures of 45-50 and 50-55 °C in the first and second stages, carried out for 3 and 2 hours, respectively, was observed to have an equivalent thickness value of 112 μm, almost half the value of 210 μm for the previous coating obtained at 45-50 and 55-60 °C. The actual effective thickness value of the coating across which gas permeation takes place

is expected to be lower than the equivalent thickness value calculated, for the substrates used in this study. Both of these coatings had sufficiently low gas permeance values lower than 10^{-9} mol/m^2.s.Pa.

Finally, the results of XRD and TGA analyses revealed that both of these coatings with low gas permeabilities were highly crystalline zeolite A coatings.

Next stages of research might focus on:

- a more detailed optimization of the system parameters, which were observed to be highly interconnected, in order to prepare even thinner coatings with low permeabilities,
- testing of the prepared coatings with chosen separation applications, such as pervaporation applications,
- improvement of the gas permeation system to make the measurement of permeance values lower than 10^{-9} mol/m^2.s.Pa possible,
- integrating seeding to the coating procedure in order to obtain fully crystalline, thinner and inter-connected zeolite coatings in shorter synthesis times, and
- possibility of improving substrate design further by using different meshes and their combinations.

REFERENCES

[1] **Barrer, R. M.** (1981). Zeolites and their synthesis. *Zeolites*, *1*(3), 130–140.

[2] **McCusker, L. B., Olson, D. H., & Baerlocher, C.** (2007). Atlas of Zeolite Framework Types. In *Atlas of Zeolite Framework Types*

[3] **Tatlier, M., Tantekin-Ersolmaz, B., & Erdem-Şenatalar, A.** (1999). A novel approach to enhance heat and mass transfer in adsorption heat pumps using the zeolite-water pair. *Microporous and Mesoporous Materials*, *27*(1), 1–10.

[4] **Mehla, S., Das, J., Jampaiah, D., Periasamy, S., Nafady, A., & Bhargava, S. K.** (2019). Recent advances in preparation methods for catalytic thin films and coatings. *Catalysis Science and Technology*, *9*(14), 3582–3602.

[5] **Maraş, T.** (2015). Geniş metal destekler üzerinde zeolit kaplamalarının hazırlanması ve karakterizasyonu, *Yüksek Lisans Tezi*, İ.T.Ü. Fen Bilimleri Enstitüsü, İstanbul.

[6] **Erdem-Senatalar, A., Tatlier, M., & Ürgen, M.** (1999). Preparation of zeolite coatings by direct heating of the substrates. *Microporous and Mesoporous Materials*, *32*(3), 331–343.

[7] **Maraş, T., Nerat, E. Y., Erdem, A., & Tatlier, M**. (2021). Preparation of zeolite coatings by induction heating of the substrate. *Journal of Sol-Gel Science and Technology*, *98*(1), 54–67.

[8] **Davis, M. E.** (1991). Zeolites and Molecular Sieves: Not Just Ordinary Catalysts. *Industrial and Engineering Chemistry Research*, *30*(8), 1675–1683.

[9] **Perego, C., & Carati, A.** (2008). Zeolites and zeolite-like materials in industrial catalysis. In *Zeolites* (Vol. 661, Issue 2).

[10] **Breck, D.W.** (1984). Zeolite Molecular Sieves: Structure, Chemistry, and Use, *R.E. Krieger, Malabar, Fla.,* 593, 634–636, 654

[11] **Nakano, Takehito & Nozue, Yasuo.** (2007). Orbital degeneracy and magnetic properties of potassium clusters incorporated into nanoporous crystals of zeolite A. *Journal of Computational Methods in Sciences and Engineering. 7.* 443-462.

[12] **Martinez, C., Perez, J.,** 2011. Zeolites and Ordered Porous Solids: Fundamentals and Applications, *3rd FEZA School Organizing Committee*, Universidad Politecnica de Valencia, Spain, July 8-9.

[13] **Yu, J.,** 2007. Chapter 3 Synthesis of zeolites, *Introduction to Zeolite Science and Practice,* 39-103.

[14] **Kostinko, J. A.** (1982). Factors Influencing the Synthesis of Zeolites A, X, and Y. *American Chemical Society, Division of Petroleum Chemistry, Preprints*, *27*(2), 487–450.

[15] **Jansen, J.C., Kaschiev, D., Erdem-Senatalar, A.** (1994). Preparation of coatings of molecular sieve crystals for catalysis and separation, in: *J.C. Jansen, M. Stöcker, H.G. Karge, J. Weitkamp (Eds.), Stud. Surf. Sci. Catal. 85*, 215–250, Elsevier, Amsterdam.

[16] **Jansen, J.C., Coker, E.N. (**1996). Zeolitic membranes, Curr. *Opin. Solid State Mater. Sci. 1*, 65–68.

[17] **Wenqin, P., Ueda, S., & Koizumi, M.** (1986). The synthesis of zeolite NaA from homogeneous solutions and studies of its properties. In *Studies in Surface Science and Catalysis* (Vol. 28, Issue C). Kodansha Ltd.

[18] **Pina, M. P., Mallada, R., Arruebo, M., Urbiztondo, M., Navascués, N., De La Iglesia, O., & Santamaria, J.** (2011). Zeolite films and membranes. Emerging applications. *Microporous and Mesoporous Materials*, *144*(1–3), 19–27.

[19] **Arruebo, M., Mallada, R., Santamaria, J., Cejka, J., Peréz-Pariente, J., Roth, W.J.** (2008). Zeolites: From *Model Materials to Industrial Catalysts, Transworld Research Network, Trivandrum*, 125–250.

[20] **Wenten, I. G., Dharmawijaya, P. T., Aryanti, P. T. P., Mukti, R. R., & Khoiruddin.** (2017). LTA zeolite membranes: Current progress and challenges in pervaporation. *RSC Advances*, *7*(47), 29520–29539.

[21] **Basak, S., Kundu, D., & Naskar, M. K.** (2014). Low temperature synthesis of NAA zeolite membranes: The effect of primary and secondary crystallizations. *Ceramics International, 40(8),* 12923–12930.

[22] **Aguado, S., Gascon, J., Farrusseng, D., Jansen, J. C., & Kapteijn, F.** (2011). Simple modification of macroporous alumina supports for the fabrication of dense NAA zeolite coatings: Interplay of electrostatic and Chemical Interactions. *Microporous and Mesoporous Materials, 146(1-3)*, 69–75.

[23] **Aguado, S., Gascón, J., Jansen, J. C., & Kapteijn, F.** (2009). Continuous synthesis of NAA zeolite membranes. *Microporous and Mesoporous Materials, 120(1-2),* 170–176.

[24] **Li, Y., Chen, H., Liu, J., & Yang, W.** (2006). Microwave synthesis of LTA zeolite membranes without seeding. *Journal of Membrane Science, 277(1-2*), 230–239.

[25] **Huang, A., & Yang, W.** (2007). Hydrothermal synthesis of NAA zeolite membrane together with microwave heating and conventional heating. *Materials Letters, 61(29),* 5129–5132.

[26] **Huang, A., Yang, W., & Liu, J.** (2007). Synthesis and pervaporation properties of NAA zeolite membranes prepared with vacuum-assisted method. *Separation and Purification Technology, 56(2*), 158–167.

[27] **Moheb Shahrestani, M., Moheb, A., & Ghiaci, M.** (2013). High performance dehydration of ethyl acetate/water mixture by pervaporation using NAA zeolite membrane synthesized by vacuum seeding method. *Vacuum, 92,* 70–76.

[28] **Sato, K., & Nakane, T.** (2007). A high reproducible fabrication method for industrial production of high flux NaA zeolite membrane. *Journal of Membrane Science, 301(1–2),* 151–161.

[29] **Wang, Z., Ge, Q., Gao, J., Shao, J., Liu, C., & Yan, Y**. (2011). High-performance zeolite membranes on inexpensive large-pore supports: Highly reproducible synthesis using a seed paste. *ChemSusChem, 4(11)*, 1570–1573.

[30] **Huang, A., Lin, Y. S., & Yang, W.** (2004). Synthesis and properties of A-type zeolite membranes by secondary growth method with vacuum seeding. *Journal of Membrane Science, 245(1–2),* 41–51.

[31] **Shao, J., Ge, Q., Shan, L., Wang, Z., & Yan, Y.** (2011). Influences of Seeds on the Properties of Zeolite NaA Membranes on Alumina Hollow Fibers. *Industrial & Engineering Chemistry Research, 50(16),* 9718–9726.

[32] **Mintova, S., Olson, N. H., Valtchev, V., & Bein, T.** (1999). Mechanism of Zeolite A Nanocrystal Growth from Colloids at Room Temperature. *Science, 283(5404),* 958–960.

[33] **Kochkodan, V., & Hilal, N.** (2015). A comprehensive review on surface modified polymer membranes for biofouling mitigation. *Desalination. 356.*

[34] **Fedosov, D. & Smirnov, A. & Knyazeva, E. & Ivanova, I..** (2012). Zeolite Membranes: Synthesis, Properties, and Application. *Petroleum Chemistry. 51.*

[35] **Mahdi, T., & Ahmad, A., & Nasef, M., & Ripin, A.** (2015). State-of-the-Art Technologies for Separation of Azeotropic Mixtures. *Separation and Purification Reviews. 44.*

[36] **Daramola, M.O. & Aransiola, Elizabeth & Ojumu, Tunde.** (2012). Potential Applications of Zeolite Membranes in Reaction Coupling Separation Processes. *Materials. 5*. 2101-2136.

[37] **Url-1** *<https://www.erkanlar.com.tr/images/katalog.pdf>*, date retrieved 10.01.2022.

[38] **Url-2** *<https://www.jbweld.com/product/j-b-weld-twin-tube>,* date retrieved 10.01.2022.

[39] **Leung, K. M., Edwards, P. P., Jones, E., & Sartbaeva, A. (2015).** Microwave synthesis of LTN framework zeolite with no organic structure directing agents. *RSC Advances, 5(45),* 35580-35585.

APPENDICES

APPENDIX A. Results of Calibration Experiments

Results of calibration experiments obtained for 24x110/500 and 24x1110/500/500 type substrates are given in Table A.1 and Table A.2. Flow rate was kept at 149.6 mL/min in these experiments.

Table A.1 : Calibration results obtained using 24x110/500 type substrate.

Induction power (kW)	Flow rate (ml/min)	Cryostatic water bath temperature (°C)	Ambient temperature (°C)	Reactor inlet temperature (°C)	Reactor outlet temperature (°C)	Difference between inlet-outlet temperatures (°C)
4.5	149.6	5	30.5	45.4	52.8	7.4
4.0	149.6	5	31.0	41.0	46.0	6.0
3.5	149.6	5	31.0	36.4	41.2	4.8
3.0	149.6	5	29.5	32.3	36.2	3.9
4.5	149.6	10	30.5	47.7	55.0	7.3
4.0	149.6	10	30.5	43.3	49.3	6.0
3.5	149.6	10	29.0	39.5	44.1	4.6
3.0	149.6	10	29.0	35.5	39.4	3.9
4.5	149.6	20	29.5	52.9	60.4	7.5
4.0	149.6	20	30.0	48.7	54.6	5.9
3.5	149.6	20	30.0	44.7	49.4	4.7
3.0	149.6	20	29.0	40.4	44.3	3.9
4.5	149.6	30	31.0	58.3	65.7	7.4
4.0	149.6	30	30.5	54.1	60.1	6.0
3.5	149.6	30	30.5	50.2	54.9	4.7
3.0	149.6	30	30.0	46.2	50.2	4.0

Table A.2 : Calibration results obtained using 24x110/500/500 type substrate.

Induction power (kW)	Flow rate (ml/min)	Cryostatic water bath temperature (°C)	Ambient temperature (°C)	Reactor inlet temperature (°C)	Reactor outlet temperature (°C)	Difference between inlet-outlet temperatures (°C)
4.5	149.6	5	31.5	43.7	50.9	7.2
4.0	149.6	5	32.5	40.7	46.4	5.7
3.5	149.6	5	33.0	35.6	40.2	4.6
3.0	149.6	5	33.5	31.1	34.7	3.6
4.5	149.6	10	32.5	45.7	52.8	7.1
4.0	149.6	10	32.5	40.9	46.7	5.8
3.5	149.6	10	32.0	37.7	42.3	4.6
3.0	149.6	10	31.0	33.6	37.2	3.6
4.5	149.6	20	29.5	50.9	58.4	7.5
4.0	149.6	20	30.0	46.4	52.1	5.7
3.5	149.6	20	31.0	42.6	47.0	4.4
3.0	149.6	20	29.5	38.6	42.2	3.6
4.5	149.6	30	30.0	55.9	63.3	7.4
4.0	149.6	30	30.0	51.9	57.5	5.6
3.5	149.6	30	30.5	48.4	52.9	4.5
3.0	149.6	30	32.0	44.0	47.7	3.7

For the substrate type 24x110/200x1400, synthesis experiments were planned at three different flow rates. Thus, calibration experiments were repeated for each of these flow rates. Results obtained can be seen in Table A.3, Table A.4 and Table A.5.

Table A.3 : Calibration results obtained using 24x110/200x1400 type substrate (Flow rate: 224.4 ml/min).

Induction power (kW)	Flow rate (ml/min)	Cryostatic water bath temperature (°C)	Ambient temperature (°C)	Reactor inlet temperature (°C)	Reactor outlet temperature (°C)	Difference between inlet-outlet temperatures (°C)
5.0	224.4	5	32.5	50.9	57.2	6.3
4.5	224.4	5	33.5	46.4	51.9	5.5
4.0	224.4	5	33.0	41.1	45.9	4.8
3.5	224.4	5	31.0	36.9	41.2	4.3
5.0	224.4	10	33.0	55.1	61.6	6.5
4.5	224.4	10	31.5	50.0	55.7	5.7
4.0	224.4	10	31.0	45.1	49.9	4.8
3.5	224.4	10	31.5	40.3	44.6	4.3
5.0	224.4	20	32.5	62.4	68.8	6.4
4.5	224.4	20	33.0	57.6	63.3	5.7
4.0	224.4	20	32.0	52.5	57.4	4.9
3.5	224.4	20	32.0	46.9	51.2	4.3

Table A.4 : Calibration results obtained using 24x110/200x1400 type substrate (Flow rate: 149.6 ml/min).

Induction power (kW)	Flow rate (ml/min)	Cryostatic water bath temperature (°C)	Ambient temperature (°C)	Reactor inlet temperature (°C)	Reactor outlet temperature (°C)	Difference between inlet-outlet temperatures (°C)
4.5	149.6	5	31.0	45.3	53.1	7.8
4.0	149.6	5	31.0	40.2	46.8	6.6
3.5	149.6	5	31.5	36.0	41.8	5.8
3.0	149.6	5	31.5	31.3	35.8	4.5
4.5	149.6	10	33.5	47.4	54.6	7.2
4.0	149.6	10	31.5	43.7	50.4	6,7
3.5	149.6	10	31.5	38.9	44.7	5.8
3.0	149.6	10	31.5	34.8	39.3	4.5
4.5	149.6	20	29.5	56.5	64.0	7.5
4.0	149.6	20	31.0	51.1	57.8	6.7
3.5	149.6	20	30.5	46.0	51.6	5.6
3.0	149.6	20	29.5	41.2	45.8	4.6

Table A.5 : Calibration results obtained using 24x110/200x1400 type substrate (Flow rate: 74.8 ml/min).

Induction power (kW)	Flow rate (ml/min)	Cryostatic water bath temperature (°C)	Ambient temperature (°C)	Reactor inlet temperature (°C)	Reactor outlet temperature (°C)	Difference between inlet-outlet temperatures (°C)
4.0	74.8	5	32.5	39.9	48.8	8.9
3.5	74.8	5	31.0	35.1	42.8	7.7
3.0	74.8	5	31.5	30.7	37.0	6.3
2.5	74.8	5	29.0	24.8	30.2	5.4
4.0	74.8	10	33.5	43.5	52.2	8.7
3.5	74.8	10	33.5	37.9	45.7	7.8
3.0	74.8	10	33.0	33.6	40.0	6.4
2.5	74.8	10	33.0	27.4	32.7	5.3
4.0	74.8	20	31.5	50.6	59.4	8.8
3.5	74.8	20	32.0	45.0	52.7	7.7
3.0	74.8	20	32.0	39.7	46.2	6.5
2.5	74.8	20	33.0	35.2	40.5	5.3

APPENDIX B: XRD Results

XRD results of the samples taken from the inner and outer surfaces are compared in Figure B.1.a and B.1.b, for the coatings obtained from A2 and A3, respectively.

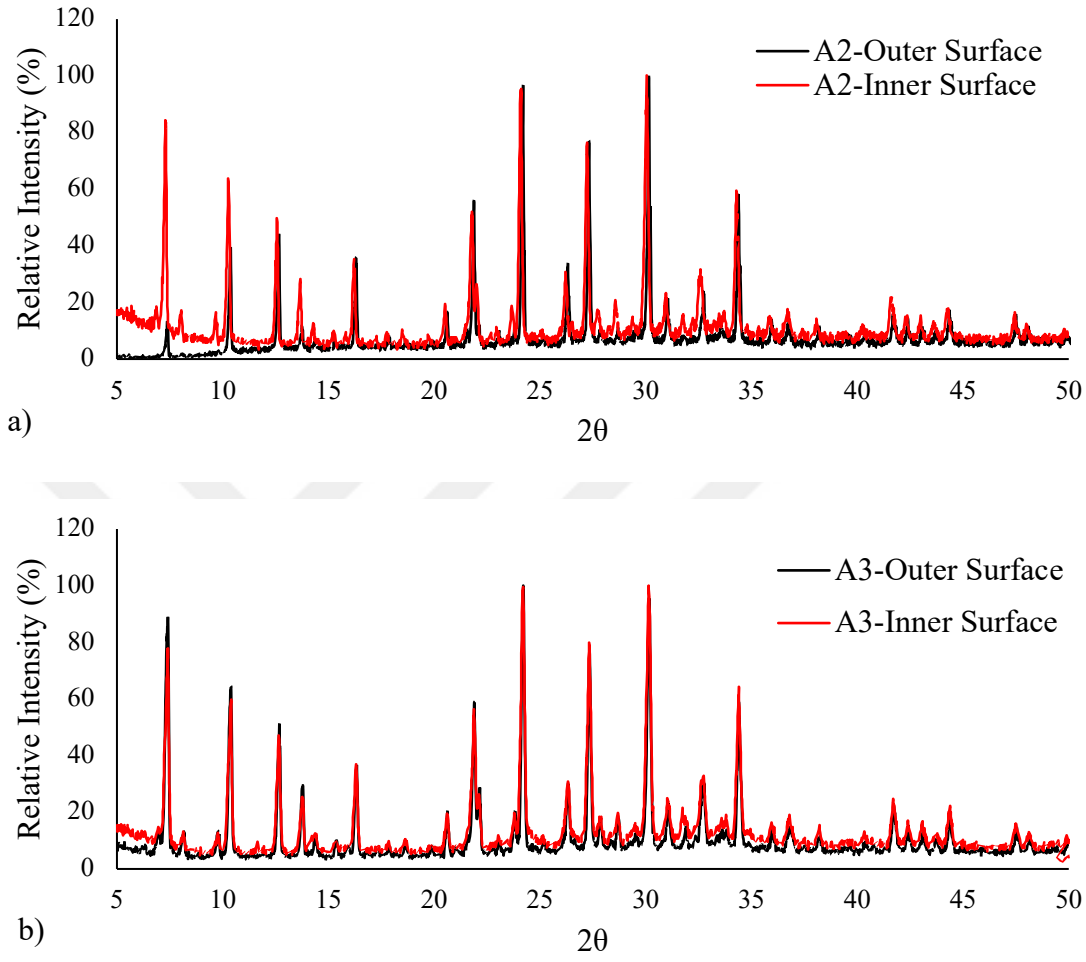

Figure B.1 : Comparison of XRD results of the samples taken from the inner and outer surface of the substrate coated in experiment a) A2 and b) A3.

Effect of synthesis time on the XRD results of the samples taken from the outer and inner surfaces of the coatings are compared in Figures B.2.a and B.2.b, respectively.

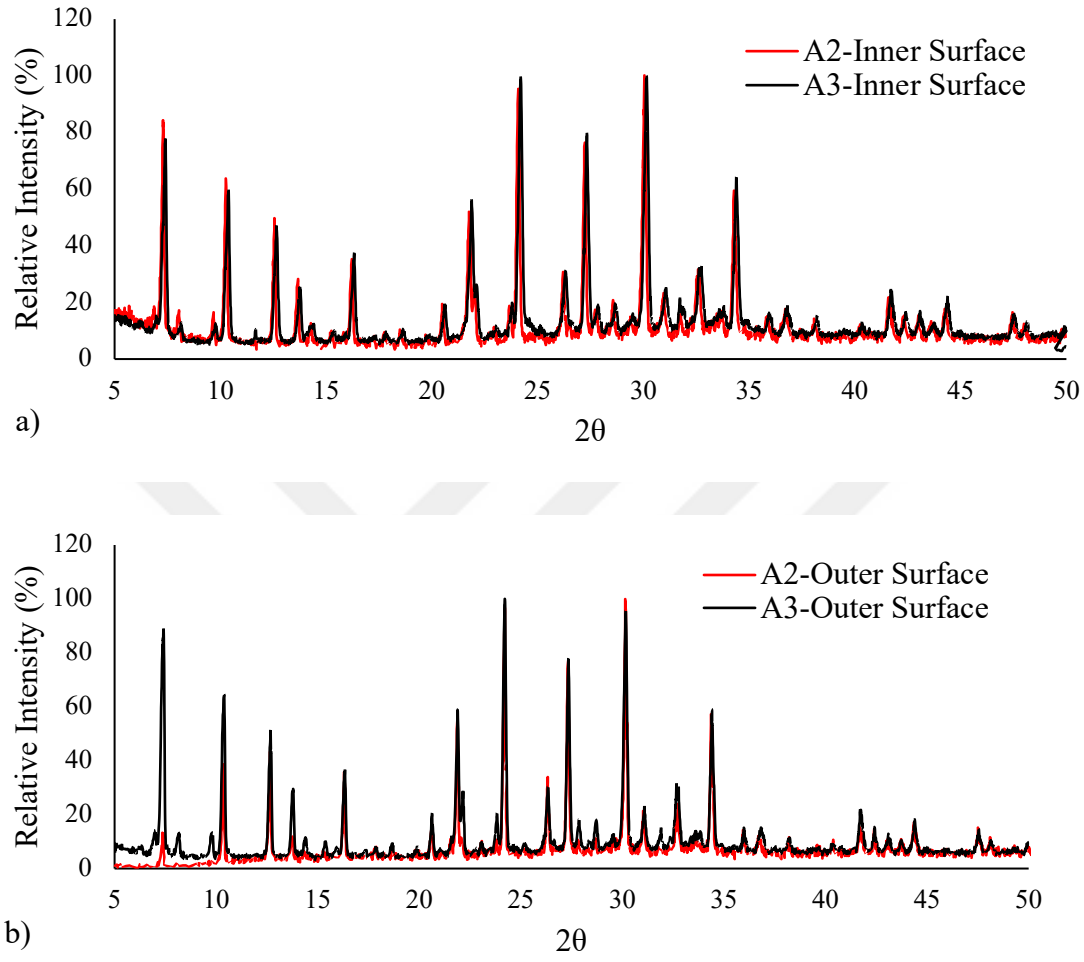

Figure B.2 : Comparison of XRD results of the samples taken from the a) inner and b) outer surfaces of the substrates coated in experiment A2 and A3.

XRD results of the samples taken from the inner and outer surfaces of A5 and A6 are compared in Figure B.3.

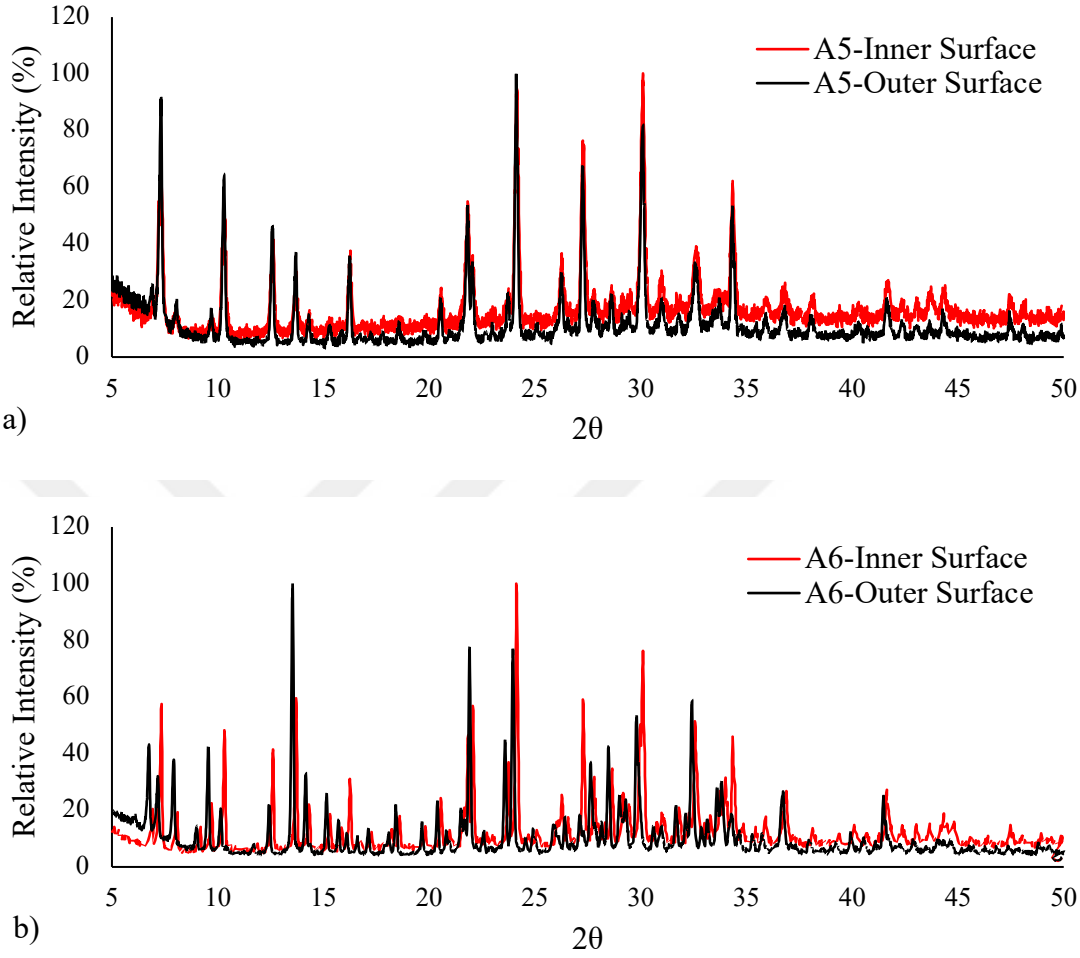

Figure B.3 : Comparison of XRD results of the samples taken from the inner and outer surface of the substrate coated in experiment a) A5 and b) A6.

Effect of synthesis time on the XRD results of the samples taken from the inner and outer surfaces of the coatings, are compared in Figures B.4.a and B.4.b, respectively.

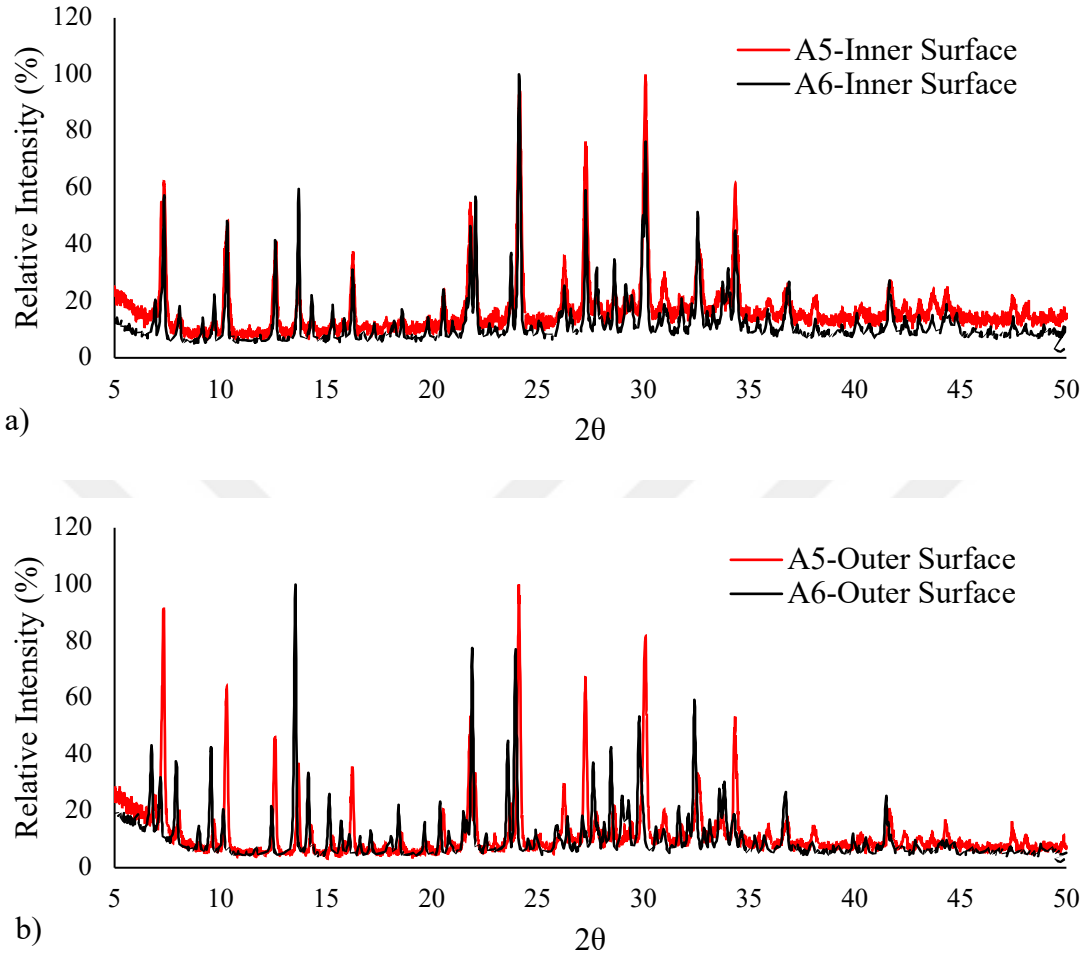

Figure B.4 : Comparison of XRD results of the samples taken from the a) inner and b) outer surfaces of the substrates coated in experiment A5 and A6.

Figures B.5.a and B.5.b show the effect of substrate type on the coatings obtained after 3 hours of synthesis, for the samples taken from the outer and inner surfaces, respectively.

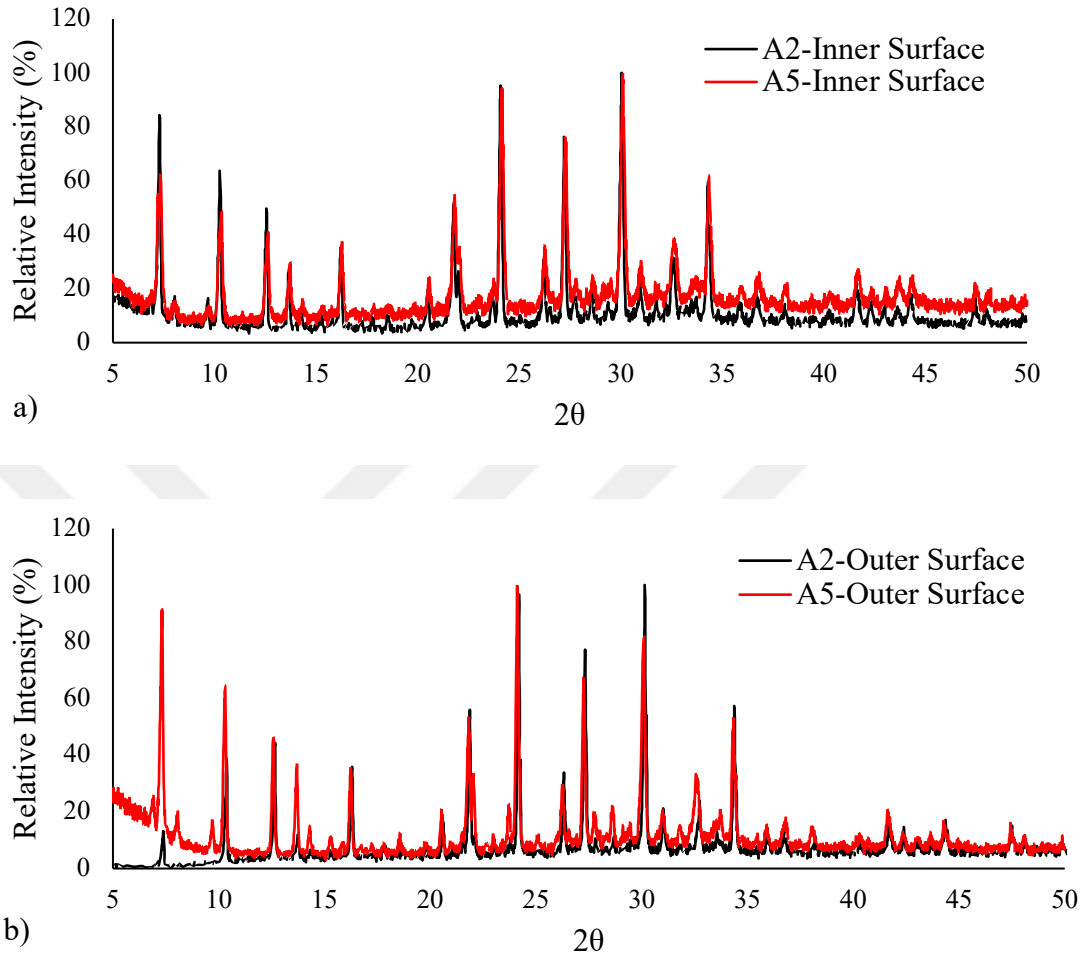

Figure B.5 : Comparison of XRD results of the samples taken from the a) inner and b) outer surfaces of the substrates coated in experiment A2 and A5.

Figures B.6.a and B.6.b show the effect of substrate type on the coatings obtained after 5 hours of synthesis, for the samples taken from the outer and inner surfaces, respectively.

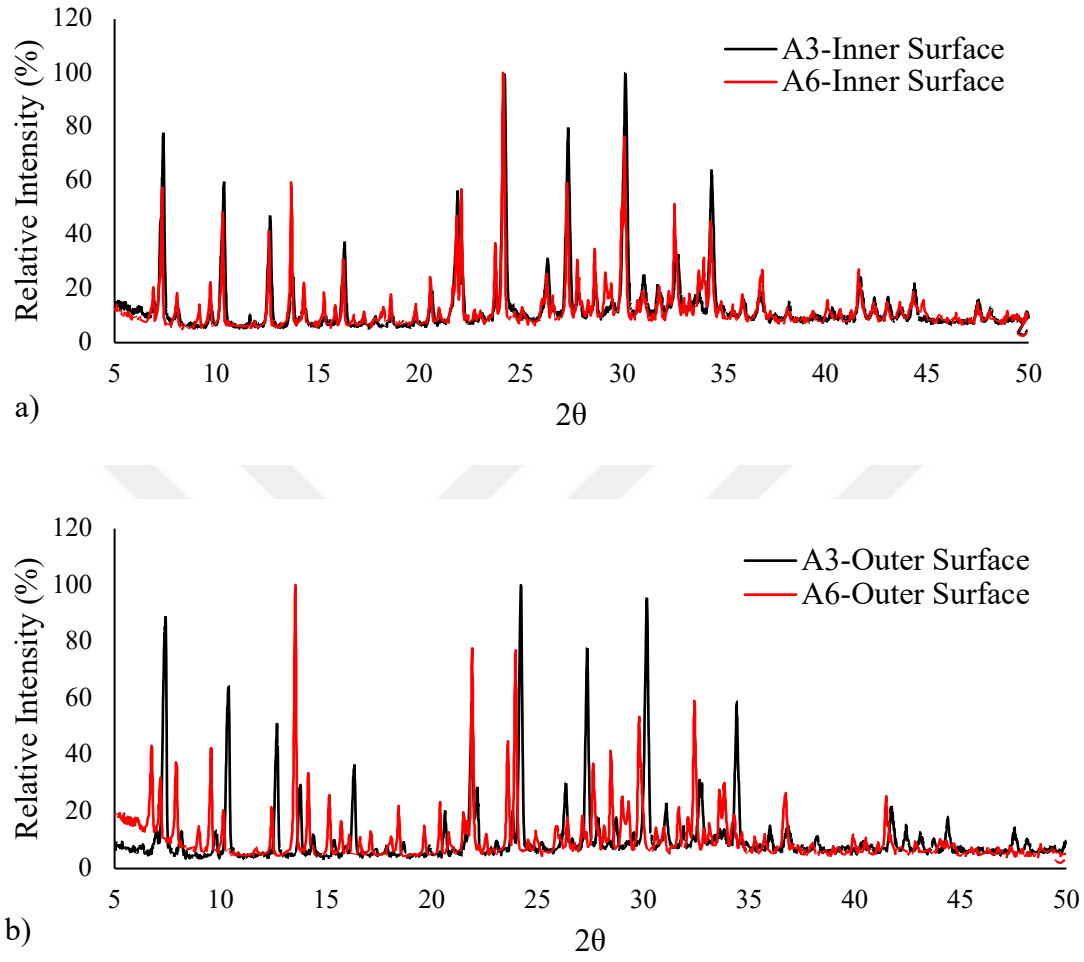

Figure B.6 : Comparison of XRD results of the samples taken from the a) inner and b) outer surfaces of the substrates coated in experiment A3 and A6